

**Renormalization approach to constituent quark models of quarkonium**J. Segovia,<sup>1,\*</sup> D. R. Entem,<sup>1,†</sup> F. Fernández,<sup>1,‡</sup> and E. Ruiz Arriola<sup>2,3,§</sup><sup>1</sup>*Grupo de Física Nuclear and IUFFyM, Universidad de Salamanca, E-37008 Salamanca, Spain*<sup>2</sup>*Departamento de Física Atómica, Molecular y Nuclear, Universidad de Granada, E-18071 Granada, Spain*<sup>3</sup>*Instituto Carlos I de Física Teórica y Computacional, Universidad de Granada, E-18071 Granada, Spain*

(Received 6 August 2011; revised manuscript received 3 February 2012; published 2 April 2012)

Constituent quark models, while successful, require a great deal of fine-tuning of the short-distance interactions by introducing phenomenological gluonic form factors which are ultimately designed to accurately reproduce the spectrum. We apply and develop renormalization ideas to reduce the short-distance sensitivity and show that, as naively expected, but not explicitly implemented in the models, the physics of binding is entirely linked to the string tension whereas leptonic decays depend more on the gluon exchange potential. We also show how the spectrum of  $S$ - and  $D$ - $1^{--}$  states is successfully intertwined through the singular tensor interaction.

DOI: 10.1103/PhysRevD.85.074001

PACS numbers: 14.40.Pg, 11.10.Gh, 12.39.Pn

**I. INTRODUCTION**

After the discovery of the first heavy-quark bound states, the  $\psi$  and the  $Y$  systems, it was soon realized that a nonrelativistic picture seemed to hold for them. Since then, the charmonium system has become the prototypical “hydrogen atom” of meson spectroscopy and therefore it was the first and simplest case where a bound state of quarks could be studied. The old Cornell potential [1]

$$V(r) = -\frac{4\alpha_s}{3r} + \sigma r \quad (1)$$

provides a rough estimate of the  $1^{--}$  charmonium spectrum and, in particular, of the  $J/\psi$  resonance (see e.g. Refs. [2,3] for a review and references therein). In potential models, One-Gluon Exchange (OGE) short-distance singularities appear and phenomenological gluonic form factors must be introduced (see e.g. [4] for an early proposal). This triggers an unpleasant short-distance sensitivity, and as we will show it mainly hides the fact that the ground state is actually being used as an input rather than a prediction. In this paper we want to make this statement more quantitative and to analyze to what extent can one disentangle the physics of the ground state to that of the excited states. The method which we will be using is based on renormalization ideas. Actually, after imposing an ultraviolet cutoff we require a natural renormalization condition, namely, we fix the  $J/\psi$  mass while varying the cutoff. In this way we aim to embody short-distance insensitivity which proves useful in the description of excited states and sidesteps the well-known ambiguities of the short-distance potentials. The presence of long-range confining forces suggests pursuing the calculations in coordinate space. To provide a proper and broad

perspective and to avoid confusion with other approaches closely related, it is of interest to review some relevant and related developments in what follows.

For the lowest-lying bound states the size of the system is smaller or comparable than  $1/\Lambda_{\text{QCD}}$  [5,6], whereas excited states start feeling the long range string tension. In the case of charmonium this is so until one reaches the  $\bar{D}D$  production threshold. Of course, one expects that at short distances corrections are computable within perturbation theory due to asymptotic freedom, whereas at long distances one must resort to lattice calculations.

For heavy particles the static energy,  $E(R) - 2m$ , is an observable and thus a gauge and scale independent quantity. The rigorous nonperturbative definition of the  $\bar{Q}Q$  potential is the expectation value of the Wilson loop and has been continuously used on lattice calculations (a review on potentials from lattice QCD can be found e.g. in Ref. [7]). It should be noticed that potentials are computed for point-like sources, i.e. structureless quarks. The determination of the  $\bar{Q}Q$  potential has been carried out in perturbation theory up to  $N^3\text{LO}$  [8,9]. Looking for a scale independent potential generates the Renormalon problem (for a review see e.g. Ref. [10]) which causes serious convergence difficulties. Effective Field Theory (EFT) methods disentangle the hard, soft, and ultrasoft scales perturbatively [11] and explicitly solve the problem.<sup>1</sup>

The pNRQCD approach [12,13] is an EFT which has better convergence properties than NRQCD since it encodes the ultrasoft scales nonperturbatively in terms of

<sup>1</sup>We remind that the NRQCD charmonium is a hydrogen-like state which is modified by subsequent corrections. The internal consistency of such an approach does not necessarily imply that confining forces are irrelevant for the discussion of excited states. Actually our main point is that as long as the ground state is properly accounted for we expect all these corrections to be largely irrelevant. Thus there is no contradiction between adopting a NRQCD view point for the ground state and our view point for the excited states.

\*segonza@usal.es

†entem@usal.es

‡fdz@usal.es

§earriola@ugr.es

potentials which enter as Wilson coefficients and should be obtained directly from the lattice or string models enabling a reliable description of excited states. The bottom line seems to be that perturbative potentials should be treated perturbatively whereas nonperturbative potentials should be treated nonperturbatively.

Following an observation [14] that the renormalon problem is triggered by an illegal extension of Fourier integrals to all momenta, a parametrization of the lattice data in the short-distance region,  $r \leq 0.15$  fm, has been proposed [15] cutting off low momenta below  $\mu_f \sim 1$  GeV. If  $\mu_f \rightarrow 0$  a flagrant lack of convergence of perturbation theory has been pictorially represented in Ref. [15]; depending on the scheme proposed one may even violate fundamental inequalities [16,17]. It should be noted that this representation smoothly matches the current lattice determination of the static energy allowing an analysis of the quarkonium spectrum, but suggests that the nonperturbative contribution corresponds to  $q \leq \mu_f$ , larger than the ultrasoft scales expected from pNRQCD. Unlike the  $\mu_f \rightarrow 0$  case the convergence is very good and basically a simple OGE potential is left.

Of course all these considerations could best be handled transparently from a fundamental point of view by solving the theory *ab initio*. However, direct lattice QCD calculations of quarkonium spectrum require small enough lattice spacings, so that  $Ma \ll 1$  and so far promising calculations operate at  $a \sim 0.1\text{--}0.2$  fm producing some overestimation of excited states [18].

Turning to a less fundamental approach such as the nonrelativistic quark model and in the spirit of the Cornell potential and extensions of it let us mention that the standard regularization of the short-distance contributions to the OGE potential (corresponding to delta contact interactions and the tensor and spin-orbit pieces), actually corresponds to tune the parameters of the regulator to fit the  $J/\psi$  mass. In addition, one of the usual parameters which are adjusted is the strong coupling constant,  $\alpha_s$ . However, the world average strong coupling constant is  $\alpha_s(M_{Z^0}) = 0.1184 \pm 0.0007$  [19]. The measured values of  $\alpha_s(Q^2)$ , covering energy scales from  $Q \equiv M_\tau = 1.78$  GeV to 209 GeV, exactly follow the energy dependence predicted by QCD and therefore significantly test the concept of Asymptotic Freedom. Therefore, the value of  $\alpha_s$  at the charm quark mass is fixed and is not larger than 0.2–0.3 This value contradicts some quark models.

A nonperturbative determination of the QCD potential at  $\mathcal{O}(1/m)$  was undertaken for the first time in [20,21], they found a potential which depends on the interquark distance as  $-c/r^2$  and it is comparable with the coulombic term of the static potential when applied to charmonium and amounts to one-fourth of the coulombic term for bottomonium.

Lattice calculations of  $1/m$  corrections based on the Bethe-Salpeter amplitude [22] (see also [23]) reveal that the dependence with the interquark distance of the  $1/m$

contributions to the potential is the same than in the case above but another term which grows logarithmically with  $r$  was found. When the data are fitted taking into account LO and NLO contributions to the potential, the coefficients which accompany Coulomb and string forces are comparable to those calculated through Wilson loops.

The  $\mathcal{O}(1/m^2)$  spin-dependent and momentum-dependent corrections are investigated in SU(3) lattice gauge theory [24]. These corrections are relevant ingredients of an effective field theory for heavy quarkonium called potential nonrelativistic QCD.

In the present paper we want to address the question on how much can we deduce for the charmonium spectrum from the knowledge of the potential at long distances in a way that our ignorance at short distances needs not play a crucial role. This allows to disentangle the physics of the ground state to that of the excited states which are sensitive to the perturbative (Coulomb-like) and nonperturbative (String-like) corrections. Actually, our original motivation for the present study was to analyze the role of regulators within constituent quark models like that of Ref. [25]. However, our ideas can be generally extended to any quark model and shed some light on their predictive power.

The plan of the paper is as follows. In Sec. II we provide a simplified and pedagogical discussion of our main points in the simplest case of the Cornell potential. The role of singular tensor and spin-orbit interactions is analyzed in Sec. III where an interesting correlation between  $S$ - and  $D$ -waves is found. In Sec. IV we review the bases of the constituent quark model proposed in Ref. [25]. In Sec. V we focus on the new renormalized charmonium model where the short-distance regulators have been removed as they turn out to be physically irrelevant for most observables. Interesting issues regarding the scope and applicability of these renormalization ideas are scrutinized in Sec. VI. Further aspects are dealt with by an enlightening analysis of the Bosonic String Model (BSM) in Sec. VIA. Finally, we give some conclusions in Sec. VII.

## II. RENORMALIZATION OF THE CORNELL POTENTIAL

In this section, we provide a comprehensive discussion of the renormalization approach as applied to heavy-quark systems and confining potentials within the context of nonrelativistic quantum mechanics. We extend here for confined states the discussion for scattering states carried out previously [26–28]. The Schrödinger equation is given by

$$-\frac{1}{2\mu_{\bar{q}q}}\nabla^2\Psi + V(r)\Psi = (M - m_q - m_{\bar{q}})\Psi, \quad (2)$$

where  $\mu_{\bar{q}q} = m_q m_{\bar{q}} / (m_q + m_{\bar{q}})$  is the reduced  $\bar{q} - q$  mass and the normalization condition  $\int d^3r |\Psi(\vec{r})|^2 = 1$  must be imposed on the solution. We use the standard Cornell potential

$$V(r) = -\frac{4\alpha_s}{3r} + \sigma r, \quad (3)$$

for the purposes of illustration. The more elaborated potentials, where spin-dependent corrections are added, will be discussed in later sections. It is remarkable that such a simple potential not only captures the relevant physics of the problem but also is accurately described by lattice calculations (see e.g. [29]) where Eq. (3) is favored with  $4\alpha_s/3 = 0.25(1)$ , extremely close to the BSM  $\alpha_s = \pi/16$  [30,31]. It is worth mentioning that the lattice calculations of  $\bar{q} - q$  potentials correspond to using point sources, i.e., elementary quarks until distances comparable to the lattice spacing. A smooth transition below  $a \sim 0.2$  fm towards OGE has been observed. Unless otherwise stated we will take  $\alpha_s = \pi/16$ ,  $\sigma = (420 \text{ MeV})^2 = 0.1764 \text{ GeV}^2$ ,  $M_{J/\psi} = 3096.916 \text{ MeV}$ , and  $m_c = 1200 \text{ MeV}$ .

For the spherically symmetric Cornell potential the total relative wave function can be factorized in the usual fashion,  $\Psi(\vec{r}) = (u(r)/r)Y_{lm}(\hat{r})$ , with  $u(r)$  the reduced wave function and  $Y_{lm}(\hat{r})$  the conventional spherical harmonics.

### A. Renormalization approach for bound states

Let us consider the standard nonrelativistic Schrödinger equation for bound states in  $S$ -waves

$$-\frac{1}{2\mu}u_n''(r) + V(r)u_n(r) = E_n u_n(r), \quad (4)$$

where  $u_n(r)$  vanishes at long distances and the energy is defined with respect to the  $\bar{q} - q$  threshold,  $E_n = M_n - m_q - m_{\bar{q}}$ .

Anticipating our discussion we will assume for definiteness a short-distance auxiliary cutoff,  $r_c$ , below which the potential vanishes. This cutoff is just a parameter which will ultimately be removed while keeping some physical condition fixed. Typically the range taken will be  $r_c = 0.3 - 0.01$  fm. In our case we will choose to fix the ground state energy to the experimental value. In the numerical application we will be concerned with the residual cutoff dependence of observables induced by such a procedure.

Using the standard trick of multiplying the Eq. (4) by  $u_m(r)$  and subtracting the similar equation with  $(n \leftrightarrow m)$ , we get for two different energies  $E_n \neq E_m$  the orthogonal relation between their bound state wave functions

$$\begin{aligned} & u_n'(r_c)u_m(r_c) - u_n(r_c)u_m'(r_c) \\ &= 2\mu(E_n - E_m) \int_{r_c}^{\infty} u_n(r)u_m(r)dr. \end{aligned} \quad (5)$$

Note that *usually* the regularity condition at the origin,  $u_n(r_c) = 0$  for  $r_c \rightarrow 0$ , is imposed. Whence orthogonality of wave functions with different energies holds. However, this is not the only solution to the orthogonality requirement. Instead the common boundary condition, we may as well take

$$\frac{u_m'(r_c)}{u_m(r_c)} = \frac{u_n'(r_c)}{u_n(r_c)}, \quad (6)$$

for any two states, meaning that the logarithmic derivative at short distances becomes state independent. In particular, choosing the ground state as a reference state we get the condition

$$\frac{u_0'(r_c)}{u_0(r_c)} = \frac{u_n'(r_c)}{u_n(r_c)}. \quad (7)$$

How can this logarithmic derivative be determined? If we know the energy of the ground state and the potential we may integrate from the long distance region inward to deduce  $u_0'(r_c)/u_0(r_c)$ . Once this number is known, we may use Eq. (7) to integrate out the excited state and the corresponding bound state energy can be fixed by requiring the wave function to vanish at large distances.<sup>2</sup> Thus, such a procedure allows to treat the ground state energy,  $E_0$ , as an independent variable from the potential  $V(r)$  and still deduce wave functions and the excited spectrum. There is of course the question on how to interpret the short-distance cutoff,  $r_c$ . In principle one may look for stability at scales below the relevant sizes. Actually, varying the cutoff in this region is a way of assessing theoretical uncertainties.<sup>3</sup> However, there are situations where the limit  $r_c \rightarrow 0$  is rather smooth and induces moderate changes in observables.

A good feature of the present approach is that since wave functions are matched at short distances the resulting energies are largely independent on the short-distance behavior of the potential.<sup>4</sup>

The previous discussion has been conducted for  $S$ -waves and regular potentials, i.e. fulfilling  $\lim_{r \rightarrow 0} r^2|V(r)| < \infty$ . Higher partial waves cannot be renormalized in this fashion as short distances are dominated by the centrifugal barrier. This also has the benefit of diminishing the dependence on the short-distance potential since the

<sup>2</sup>There is of course the subtlety that if we include exactly the origin the radial wave function does not provide a three-dimensional solution of the Schrödinger equation as it generates a  $\delta(\vec{x})$  term [32]. As has been discussed at length in previous works [26–28] we can take any arbitrarily small (but nonvanishing) short-distance cutoff  $r > r_c > 0$  which in the limit  $r_c \rightarrow 0^+$  generates a well-defined result. In all our discussions we assume this limiting procedure.

<sup>3</sup>In a model where phenomenological form factors are implemented *ad hoc*, just to prevent singularities, the assessment of theoretical errors could be done by choosing *all possible* regularization functions, unless the form factor is known from first principles.

<sup>4</sup>The previous approach is well documented in the mathematical literature as the theory of self-adjoint extensions of Hermitian operators. This endows the Hilbert space with a common domain of functions where the solutions of the Schrödinger equation span a complete set. The generation of a new scale independently on the potential resembles the well-known phenomenon of dimensional transmutation.

short-distance behavior of the wave function,  $u(r) \sim r^{J+1}$ , is not controlled by the potential.

The case of singular potentials has also been discussed at length (see e.g. Refs. [26–28] regarding nuclear or atomic systems). The relation to momentum space renormalization and the corresponding Lagrangian counterterms is discussed in Ref. [33]. The irrelevance of form factors is analyzed in Refs. [28,34].

## B. Analysis of the linear potential

In order to provide a clear picture of the procedure to be carried out in the present paper, we discuss the issue within the framework of the simplified model where the OGE piece is neglected. For  $S$ -wave charmonium states we have the simplified problem

$$-\frac{1}{m_c} u_{c\bar{c}}''(r) + \sigma r u_{c\bar{c}}(r) = E u_{c\bar{c}}(r). \quad (8)$$

As is well known, the general solution in the inner region is a linear combination of regular and irregular Airy functions

$$u_{c\bar{c}}(r) = c_1 \text{Ai}(z) + c_2 \text{Bi}(z), \quad (9)$$

where the dimensionless variable

$$z = \frac{m_c(-M + 2m_c + r\sigma)}{(m_c\sigma)^{2/3}} \quad (10)$$

has been introduced. At large values of the argument one has

$$\begin{aligned} \text{Ai}(z) &= \frac{e^{-2/3z^{3/2}}}{2\sqrt{\pi}z^{1/4}} [1 + \mathcal{O}(z^{-3/2})], \\ \text{Bi}(z) &= \frac{e^{2/3z^{3/2}}}{\sqrt{\pi}z^{1/4}} [1 + \mathcal{O}(z^{-3/2})], \end{aligned} \quad (11)$$

so that for bound states and assuming no opening of meson decay channels we may discard the  $\text{Bi}(z)$  function. The standard approach consists of requiring the regularity condition at the origin.

Indeed, the regular solution at the origin requires finding the zeros of the Airy function,  $\text{Ai}(z_n) = 0$ , yielding the quantization formula

$$z_n = \frac{m_c(-M_n + 2m_c)}{(m_c\sigma)^{2/3}}, \quad (12)$$

where  $z_0 = -2.33811$ ,  $z_1 = -4.08795$ ,  $z_2 = -5.52056$ ,  $z_3 = -6.78671$ ,  $z_4 = -7.94413, \dots$  are the corresponding lowest zeros. Note that in this particular case the string tension and the quark mass determine the binding energy completely.

An alternative procedure might be as follows. Since we want to fit the  $J/\psi$  mass and we are confident that the long distance dynamics is given by the linear potential [7], we are quite certain that at long distances the wave function is given by

$$u_{c\bar{c}}(r) = c_1 \text{Ai}(z), \quad (13)$$

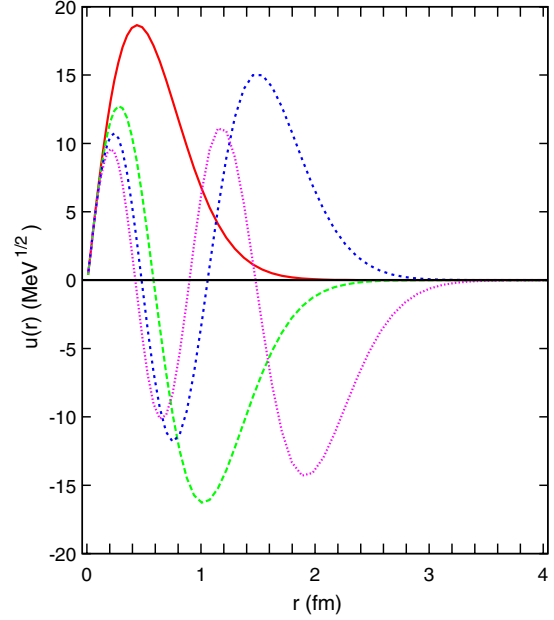


FIG. 1 (color online). Wave functions for the different states. The normalization is such that at the matching point,  $r_c \rightarrow 0$  fm, the functions and derivatives of the different states coincide.

where now  $M_{J/\psi}$  is taken as an *input*. Of course, for a generic value of the string tension the wave function will fail to vanish at the origin (see Fig. 1). This may be seen as a drawback but the gain is in the *prediction* of the excited spectrum. This is done by matching logarithmic derivatives at the origin or at a short-distance cutoff, Eq. (7), yielding

$$\frac{\text{Ai}'(z_0)}{\text{Ai}(z_0)} = \frac{\text{Ai}'(z_n)}{\text{Ai}(z_n)}, \quad (14)$$

where  $z_n$  is given by

$$z_n = \frac{m_c(-M_n + 2m_c + \sigma r_c)}{(m_c\sigma)^{2/3}}. \quad (15)$$

This condition guarantees the orthogonality of states and provides  $M_n$  from  $M_0$  for any value of  $r_c$ . Note that by definition the short-distance behavior of the wave functions is very similar, so that even though we may not know accurately the potential at short distances there is an increasingly large cancellation. The cutoff dependence of the states is depicted in Fig. 2.<sup>5</sup> As we see, changing the scale provides a mild dependence featuring the advertised short-distance insensitivity.

## C. Inclusion of a coulombic term

In heavy-quark systems the OGE potential is considered to be a very important ingredient to provide some additional short range corrections. Here we will show that as far

<sup>5</sup>The cutoff dependence can be understood on purely analytical grounds as carried out in Appendix A for a wide class of potentials.

as binding is concerned this OGE contribution becomes almost irrelevant. Contrary to what one might naively think this is actually good news. Indeed, as we mentioned in the introduction the short-distance part of the potential is not well known even at the OGE level. If we write the OGE potential in the form  $V(r) = -4\alpha_s(\mu)/3r$ , with  $\mu$  the  $\overline{\text{MS}}$  renormalization scale and  $\alpha_s(\mu)$  the running coupling constant which at leading order is given by  $\alpha_s(\mu) = 4\pi/\beta_0 \log(\mu^2/\Lambda_{\text{QCD}}^2)$  and it is not obvious what scale should one use *a priori*. Lattice calculations display such a behavior at short distances (see the recent update where running is actually observed [35]). There have been attempts to improve on this by imposing renormalization group invariance of the potential which corresponds to replace  $\alpha_s(\mu)$  by  $\alpha_s(1/r)$ . Unfortunately such a procedure breaks down due to the appearance of renormalons (see e.g. Ref. [10,15]) which spoil a convergence pattern. At leading order this corresponds to  $r = 1/\Lambda_{\text{QCD}} \sim 0.4\text{--}0.6$  fm for  $\Lambda_{\text{QCD}} = 300\text{--}500$  MeV, the value been shifted towards smaller numbers when higher-order corrections are included [15]. In addition, there is also the problem on how far should this OGE force be extended, since it only applies to very short distances. However, one expects that as compared to the linear potential the long range effect is not crucial.

The region where OGE becomes comparable with the linear potential is  $r \sim b = \sqrt{\alpha_s/\sigma} \sim 0.2\text{--}0.3$  fm where the total potential is about  $V(r) \sim -180$  MeV. At much larger distances we may neglect the OGE component so that we may take the asymptotic behavior of Eq. (13). The resulting wave functions without and with OGE are depicted in Fig. 3. Similarly to the case without OGE the procedure is

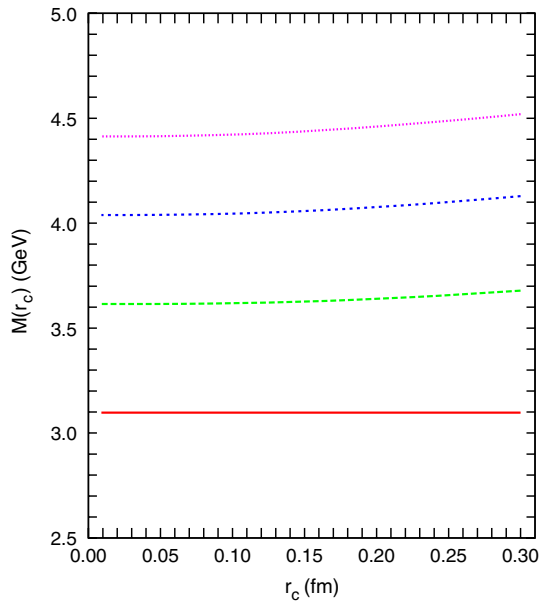


FIG. 2 (color online). Dependence of the excited charmonium states on the short-distance cutoff.

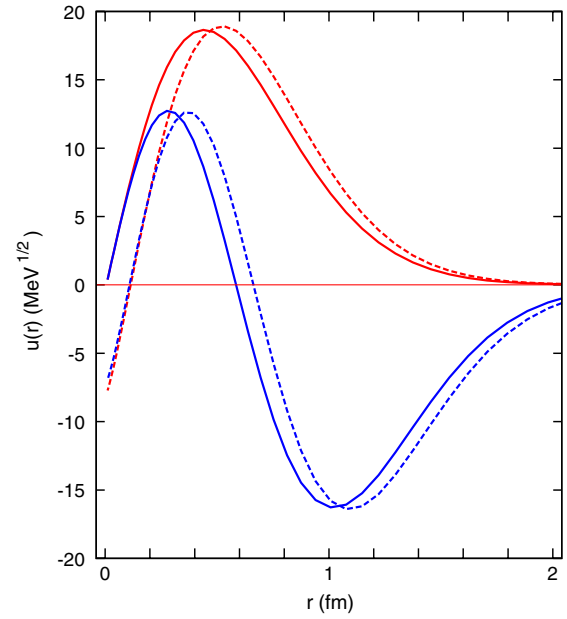


FIG. 3 (color online). Charmonium wave functions for  $\psi(1S)$  and  $\psi(2S)$  states without (solid line) and with (dashed line) One-Gluon Exchange potential.

as follows. We start from the *given* ground state energy  $M_0 = M_{J/\psi}$  integrating inward down to the short-distance cutoff radius,  $r_c$ , the full Cornell potential, Eq. (3). To facilitate the comparison we take the same asymptotic wave function for both cases, without or with OGE. As can be seen, the OGE attraction provides a larger probability in the inner region below the scale where OGE starts being negligible. Our numerical calculations indicate that this long distance scale is about 1.5 fm. From the ground state we can construct the remaining excited states by matching logarithmic derivatives at the short-distance cutoff, as indicated above.

The short-distance cutoff dependence of the excited charmonium states for several values of the strong coupling constant is similar in all cases to the  $\alpha_s = 0$  situation shown in Fig. 2. While at large  $r_c$  the calculation is dominated by the linear potential, wave functions at short distances are very much alike due to the common boundary condition. Thus, the difference in energy due to OGE comes from the energy dependence of the wave function below the nonperturbative scale. In Table I, for the case

TABLE I. Masses in MeV of  $S$ -wave charmonium states for several values of the  $\alpha_s$  coupling constant and keeping always the ground state mass  $M_0 = 3096.916$  MeV.

$n$	$\alpha_s = 0.0$	$\alpha_s = 0.1$	$\alpha_s = 0.2$	$\alpha_s = 0.3$
1	3615	3630	3638	3640
2	4039	4060	4070	4073
3	4414	4439	4449	4452
4	4756	4783	4795	4798

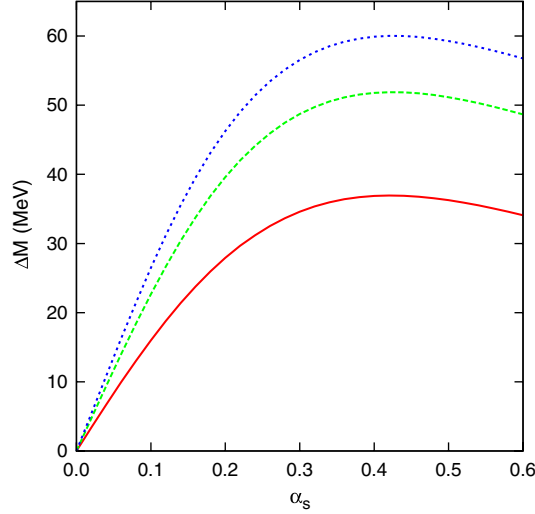


FIG. 4 (color online). Mass shift (in MeV) as a function of the strong coupling constant  $\alpha_s$  when the short-distance cutoff is removed  $r_c \rightarrow 0$  for the  $\psi(2S)$ ,  $\psi(3S)$  and  $\psi(4S)$  relative to the ground  $\psi(1S)$  state.

$r_c \rightarrow 0$ , we show numerical values of the excited states for  $\alpha_s = 0.0, 0.1, 0.2$ , and  $0.3$ . The mass shift  $\Delta M_n = M_n - M_0$  is shown in Fig. 4 for  $r_c = 0.06$  fm and as we can see the OGE effects are rather moderate.

### III. COUPLED CHANNEL SOLUTIONS: MIXING S AND D STATES

In this section we include the spin-dependent potential contributions coming from the OGE interaction to the simple Cornell potential discussed in Sec. II.

#### A. Potential

The  $\bar{q}q$  interaction can be written as

$$V(\vec{r}) = \sigma r + V_{\text{OGE}}(\vec{r}), \quad (16)$$

where now  $V_{\text{OGE}}(\vec{r})$  contains central, the coulomb interaction, and noncentral, tensor, and spin-orbit, contributions

$$V_{\text{OGE}}^C(\vec{r}) = -\frac{4\alpha_s}{3} \frac{1}{r}, \quad (17)$$

$$V_{\text{OGE}}^T(\vec{r}) = \frac{1}{3} \frac{\alpha_s}{m^2} \frac{1}{r^3} S_{12}, \quad (18)$$

$$V_{\text{OGE}}^{\text{SO}}(\vec{r}) = \frac{2\alpha_s}{m^2} \frac{1}{r^3} \vec{L} \cdot \vec{S}, \quad (19)$$

where  $\alpha_s$  is the strong coupling constant,  $m$  is the equal quark and antiquark mass,  $S_{12} = 3(\vec{\sigma}_1 \cdot \hat{r})(\vec{\sigma}_2 \cdot \hat{r}) - \vec{\sigma}_1 \cdot \vec{\sigma}_2$  is the quark tensor operator,  $\vec{S}$  the total spin operator, and  $\vec{L}$  is the relative orbital angular momentum operator.

#### B. The coupled S-D equations

Our previous discussion of renormalization was undertaken without taking into account the role played by the tensor and spin-orbit forces. In the case of charmonium, these states are a combination of  $S$  and  $D$ -wave components due to the tensor force contribution. As we will see below, this tensor force is small enough to have almost pure  $S$  and  $D$  orbital state components. The interesting aspect of our discussion below is that using just one renormalization condition we can predict all  $S$  and  $D$ -wave mesons, i.e. we reduce the number of renormalization conditions.

The radial Schrödinger equation for the  ${}^3S_1 - {}^3D_1$  coupled channel reads

$$\begin{aligned} -u''(r) + U_S(r)u(r) + U_{SD}(r)w(r) &= -\kappa^2 u(r), \\ -w''(r) + U_{SD}(r)u(r) + \left[ U_D(r) + \frac{6}{r^2} \right] w(r) &= -\kappa^2 w(r), \end{aligned} \quad (20)$$

where  $\kappa^2 = m_c(M - 2m_c)$ .  $U_S$ ,  $U_D$ , and  $U_{SD}$  are the different contributions of the reduced potential,  $U(r) = 2\mu V(r)$ , where the  ${}^3S_1 - {}^3D_1$  coupled channel potential is given by

$$\begin{aligned} V_S(r) &= -\frac{4\alpha_s}{3r} + \sigma r, \\ V_D(r) &= -\frac{4\alpha_s}{3r} + \sigma r - \frac{20}{3} \frac{\alpha_s}{m_c^2} \frac{1}{r^3}, \\ V_{SD}(r) &= \frac{2\sqrt{2}}{3} \frac{\alpha_s}{m_c^2} \frac{1}{r^3}, \end{aligned} \quad (21)$$

in which  $\alpha_s$  is the strong coupling constant,  $\sigma$  is the string tension and  $m_c$  is the quark mass. Obviously, in order to describe a bound state we seek for normalizable solutions

$$\int_0^\infty [u(r)^2 + w(r)^2] = 1, \quad (22)$$

which impose conditions on the wave functions both at infinity as well as at the origin.

The set of equations (20) must be accompanied by asymptotic conditions at infinity. As in previous sections, we have a linear potential at large distances for both channels and therefore the wave function is a linear combination of regular and irregular Airy functions. Once we have discarded the irregular function at long distances,  $\text{Bi}(z)$ , the wave functions at infinity have the following behavior:

$$u(r) \rightarrow A_S \text{Ai}(z), \quad w(r) \rightarrow A_D \text{Ai}(z), \quad (23)$$

with  $z$  defined in Eq. (10) and  $A_S$  is the normalization factor and the asymptotic  $D/S$  ratio parameter is defined by  $\eta = A_D/A_S$ . Ideally, one would integrate the Schrödinger equation taking its solutions at infinity, Eq. (23), which depend on the bound energy and  $\eta$ . The

singular structure of the problem at short distances requires a specific analysis of the coupled equations as it has been done extensively elsewhere [34] and we adapt in Appendix C for our particular case. The result amounts to integrate from infinity for the physical value of  $M_{J/\psi}$  and  $\eta$ . Generally, the solutions diverge strongly at the origin, so that the normalization of the state is precluded. However, there is a particular value of  $\eta$  which guarantees that the wave function becomes normalizable. Then, if one imposes the regularity condition at the origin one will determine  $\eta$  and therefore the wave function of the bound state. In practice, however, the converging solution is rather elusive since integrated-in solutions quickly run into diverging solutions due to the round-off errors and dominate over the converging solution.

In the rest of the section we provide some details on how can the calculation be done efficiently. According to Ref. [34] one may proceed as follows. One can impose different auxiliary short-distance boundary conditions corresponding to a choice of regular solutions at the origin

$$\begin{aligned} u(r_c) &= 0 \text{ (BC1)}, & u'(r_c) &= 0 \text{ (BC2)}, \\ w(r_c) &= 0 \text{ (BC3)}, & w'(r_c) &= 0 \text{ (BC4)}, \\ u(r_c) - \sqrt{2}w(r_c) &= 0 \text{ (BC5)}, \\ u'(r_c) - \sqrt{2}w'(r_c) &= 0 \text{ (BC6)}. \end{aligned} \quad (24)$$

All these boundary conditions must predict the same value of  $\eta$  at some value of the cutoff radius,  $r_c$ , the precise convergence value corresponds to the particular choice. As in Ref. [36] we find convergence for the boundary conditions BC5 and BC6 for larger cutoff radii, which improves the numerical results.

To calculate the  $D/S$  asymptotic ratio,  $\eta$ , it is convenient to use the superposition principle of boundary conditions [36] to write

$$u(r) = u_S(r) + \eta u_D(r), \quad w(r) = w_S(r) + \eta w_D(r), \quad (25)$$

where  $(u_S, w_S)$  and  $(u_D, w_D)$  correspond to the boundary conditions at infinity, Eq. (23), with  $A_S = 1$  and  $A_D = 0$  and with  $A_S = 0$  and  $A_D = 1$ , respectively. Through that decomposition the boundary conditions, BC1-BC6, can be rewritten as algebraic expressions for  $\eta$ . For instance, if we use the BC6 boundary condition we get

$$\eta = -\frac{u'_S(r_c) - \sqrt{2}w'_S(r_c)}{u'_D(r_c) - \sqrt{2}w'_D(r_c)}. \quad (26)$$

Once  $\eta$  has been calculated, the wave function of the bound state is completely determined by the normalization factor  $A_S$

$$u(r) = A_S(u_S + \eta u_D), \quad w(r) = A_S(w_S + \eta w_D), \quad (27)$$

in which  $A_S$  is obtained normalizing the wave function to one

$$A_S^2 \int_0^\infty [(u_S + \eta u_D)^2 + (w_S + \eta w_D)^2] dr = 1. \quad (28)$$

The above procedure can be undertaken for the ground state of the system if its energy is known. Now, if we want to calculate the excited states of the system we must impose the orthogonality condition between wave functions of states with different energy together with the regularity condition at the origin.

For a regular potential the orthogonality between wave functions of states with different energy is a property of the solutions of the Schrödinger equation and it always holds. However, if the potential contains some attractive singular contribution we have to impose explicitly the orthogonality between wave functions.

Thus, given the ground state and one excited state, the orthogonality condition can be written as

$$\int_0^\infty dr [u_0(r)u_m(r) + w_0(r)w_m(r)] = 0, \quad (29)$$

where it is useful to rewrite the above expression through a Lagrange identity

$$[u'_0 u_m - u_0 u'_m + w'_0 w_m - w_0 w'_m]_0^\infty = 0. \quad (30)$$

Note that any individual term in the integrand is actually divergent, because of the dominance of the singular solutions at the origin. At very short distances, the orthogonality between wave functions and the regularity condition of them have been imposed at a certain cutoff radius,  $r_c$ . Of course, we always check that the numerical calculation is stable against suitable changes of the short-distance cutoff so that the range  $r_c \sim 0.01\text{--}0.3$  fm is sufficient. In that situation, the orthogonality condition, Eq. (30), can be written as

$$\begin{aligned} u'_0(r_c)u_m(r_c) + w'_0(r_c)w_m(r_c) \\ = u_0(r_c)u'_m(r_c) + w_0(r_c)w'_m(r_c), \end{aligned} \quad (31)$$

and combining this expression with the corresponding one of the boundary conditions, Eq. (24), we obtain in the case of the boundary condition BC6

$$\frac{w'_m(r_c)}{\sqrt{2}u_m(r_c) + w_m(r_c)} = \frac{w'_0(r_c)}{\sqrt{2}u_0(r_c) + w_0(r_c)}, \quad (32)$$

and similarly for all other auxiliary boundary conditions. Obviously in this case the  $D/S$  mixing of the excited state is determined from the requirement of regularity at the origin

TABLE II. Different observables computed through the coupled toy model and applied to charmonium spectrum. We take  $M_{J/\psi} = 3096.916$  MeV as input.

State	M (MeV)	$\eta$	$A_s$ (fm $^{-1/2}$ )	$\langle r^2 \rangle^{1/2}$ (fm)	$P_D$ (%)
$J/\psi$	input	-0.0037	4.01	0.637	1.52
$\psi(1D)$	3577.7	-19, 71	0.084	0.93	99.91
$\psi(2S)$	3634.2	+0.015	3.05	1.05	1.24
$\psi(2D)$	3995.9	-17.73	0.104	1.29	99.84
$\psi(3S)$	4065.1	+0.028	2.66	1.40	1.15
$\psi(3D)$	4368.7	-15.70	0.12	1.60	99.75
$\psi(4S)$	4443.1	+0.039	2.44	1.70	1.12
$\psi(4D)$	4710.8	-14.09	0.13	1.88	99.65
$\psi(5S)$	4787.4	+0.048	2.29	1.98	1.14

$$\eta_m = -\frac{u'_{S,m}(r_c) - \sqrt{2}w'_{S,m}(r_c)}{u'_{D,m}(r_c) - \sqrt{2}w'_{D,m}(r_c)}. \quad (33)$$

We will also compute other observables. The results are presented in Table II. In the numerical integration a certain maximum radius has to be selected to impose the asymptotic boundary conditions. Because of the long-range coulomb force the values of the asymptotic parameters are slowly convergent and we quote the values for  $r_{\max} = 20$  fm. The corresponding wave functions can be looked up in Fig. 5.

As we see the description of the spectrum is not particularly accurate, but one should take into account that we are only providing the  $J/\psi$  mass as an input, as well as  $\alpha_s$ ,  $m_c$ , and  $\sigma$ , for which we take generally accepted values. The present analysis suggests that exploiting these ideas one may find a reduction of parameters in quark models. As we will see in later sections, rather than being a mathematical curiosity, these correlations which are unveiled by the renormalization approach actually are embodied in quark models in a much less transparent way.

#### IV. CHARMONIUM WITH FORM FACTORS

In the previous sections we have presented how one may incorporate a desirable short-distance insensitivity into several simplified models for quarkonium. In this section we give a brief description of the specific charmonium model which fits a wider and successful phenomenology (see Ref. [25] for further details) paying special attention to the form factors introduced to regulate the unpleasant short-distance singularities. Our intention is to re-analyze the model by trading these form factors into a less model-dependent set of renormalization conditions. While the model furnishes unequal quark species we will restrict for illustration purposes to the case of charmonium.

The corresponding potentials for the  $\bar{q}q$  system stem from the nonrelativistic reduction of OGE and the confinement component. We separate the central, tensor, and spin-orbit pieces, as follows:

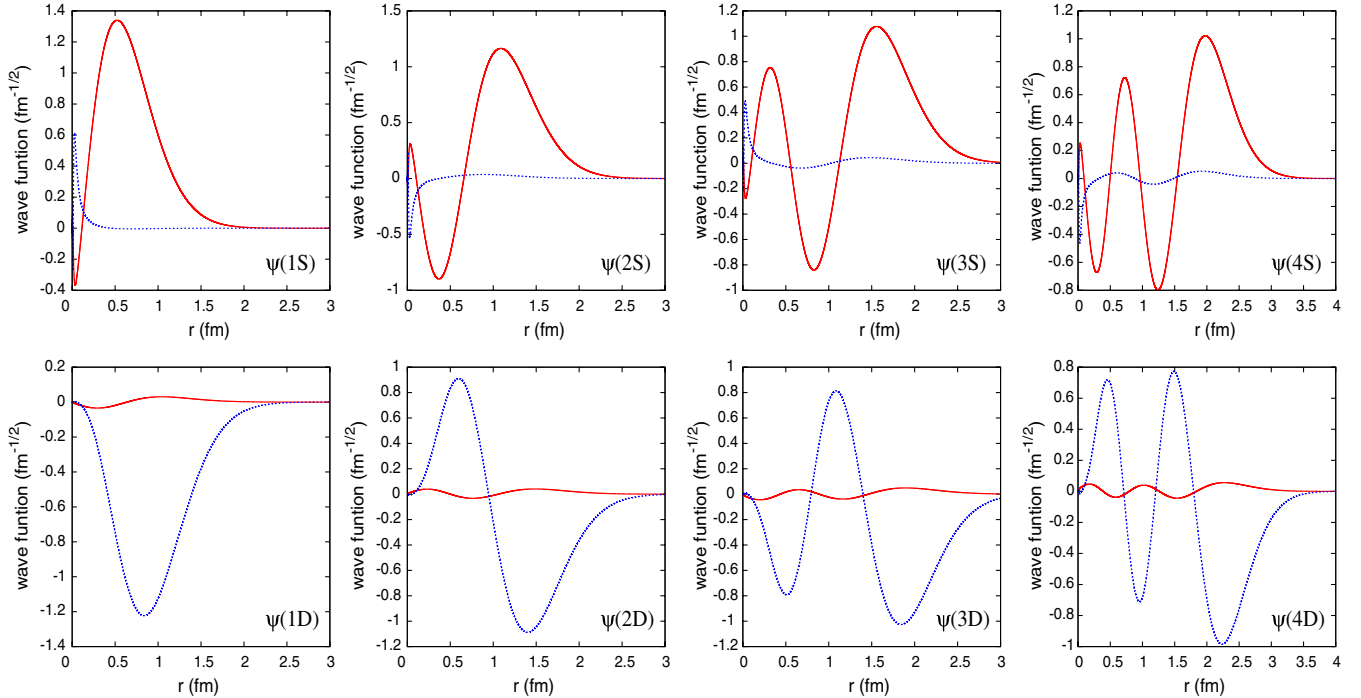


FIG. 5 (color online).  $S$  and  $D$ -wave functions of the different states of charmonium calculated through the coupled toy model.



## (i) One-Gluon Exchange

$$\begin{aligned}
V_{\text{OGE}}^C(\vec{r}) &= \frac{1}{4} \alpha_s (\vec{\lambda}_1^c \cdot \vec{\lambda}_2^c) \left[ \frac{1}{r} - \frac{1}{6m^2} (\vec{\sigma}_1 \cdot \vec{\sigma}_2) \frac{e^{-r/r_0(\mu)}}{rr_0^2(\mu)} \right], \\
V_{\text{OGE}}^T(\vec{r}) &= -\frac{1}{16} \frac{\alpha_s}{m^2} (\vec{\lambda}_1^c \cdot \vec{\lambda}_2^c) \left[ \frac{1}{r^3} - \frac{e^{-r/r_g(\mu)}}{r} \left( \frac{1}{r^2} + \frac{1}{3r_g^2(\mu)} + \frac{1}{rr_g(\mu)} \right) \right] S_{12}, \\
V_{\text{OGE}}^{\text{SO}}(\vec{r}) &= -\frac{3}{8} \frac{\alpha_s}{m^2} (\vec{\lambda}_1^c \cdot \vec{\lambda}_2^c) \left[ \frac{1}{r^3} - \frac{e^{-r/r_g(\mu)}}{r^3} \left( 1 + \frac{r}{r_g(\mu)} \right) \right] \vec{L} \cdot \vec{S}.
\end{aligned} \tag{34}$$

## (ii) Confinement

$$V_{\text{CON}}^C(\vec{r}) = [-a_c(1 - e^{-\mu_c r}) + \Delta](\vec{\lambda}_1^c \cdot \vec{\lambda}_2^c), \quad V_{\text{CON}}^{\text{SO}}(\vec{r}) = -(\vec{\lambda}_1^c \cdot \vec{\lambda}_2^c) \frac{a_c \mu_c e^{-\mu_c r}}{4m^2 r} (6 - 8a_s) \vec{L} \cdot \vec{S}, \tag{35}$$

where  $r_0(\mu) = \hat{r}_0 \frac{\mu_{mn}}{\mu}$  and  $r_g(\mu) = \hat{r}_g \frac{\mu_{mn}}{\mu}$  are short-distance regulators,  $\mu$  stands for the reduced quark mass, and  $\lambda_i^c$  are the color Gell-Mann matrices. The contact term of the central potential of one-gluon exchange is regularized in a suitable way by replacing the Dirac delta function by a Yukawa form

$$\delta(\vec{r}) \rightarrow \frac{1}{4\pi r_0^2} \frac{e^{-r/r_0}}{r}. \tag{36}$$

In Table III we show the model parameters constrained by the light quark phenomenology and also appear in the potentials operating in the heavy-quark sector.

Regarding the confinement interaction,<sup>6</sup>  $\Delta$  is a global constant adjusted to fit the origin of energies,  $a_c$  and  $\mu_c$  are model parameters. At short distances this potential presents a linear behavior with an effective confinement strength  $\sigma = -a_c \mu_c (\vec{\lambda}_1^c \cdot \vec{\lambda}_2^c)$  while it becomes constant at large distances. This type of potential shows a threshold defined by

$$V_{\text{thr}} = \{-a_c + \Delta\} (\vec{\lambda}_1^c \cdot \vec{\lambda}_2^c). \tag{37}$$

By construction, no  $\bar{q}q$  bound states can be found for energies higher than this threshold. Actually, the potential suffers a transition from a color string configuration between two static color sources into a pair of static mesons due to the breaking of the color flux-tube and the most favored subsequent decay into hadrons. In a more general setup, a dynamical coupling to the formed meson pair should be included.

<sup>6</sup>Our expressions imply the validity of Casimir scaling both for the perturbative (tree level) as well as the nonperturbative (confinement) contributions to the potential. A recent perturbative calculation to three loops displays violations to this Casimir scaling [37], although nothing is implied for the nonperturbative contribution.

The wide energy range covered by a consistent description of light, strange, and heavy mesons requires an effective scale-dependent strong coupling constant that cannot be obtained from the usual one-loop expression of the running coupling constant which diverges at  $Q^2 = \Lambda_{\text{QCD}}^2$ . Following previous work [25], we use a frozen coupling constant such as

$$\alpha_s(\mu) = \frac{\alpha_0}{\ln\left(\frac{\mu^2 + \mu_0^2}{\Lambda_0^2}\right)}, \tag{38}$$

where  $\mu$  is the reduced mass of the  $\bar{q}q$  pair and  $\alpha_0$ ,  $\mu_0$ , and  $\Lambda_0$  are parameters of the model determined by a global fit to the hyperfine splitting from the light to the heavy-quark sector. In our case this yields a value of  $\alpha_s = 0.288$ .

We note that the regulators in the tensor and spin-orbit terms of the one-gluon exchange potential as well as the smeared  $\delta$ -function of the central component are introduced just because tensor and spin-orbit terms become singular at short distances. As a consequence the collapse of the system which would occur for the pure unregularized  $\delta$ -function is prevented. The previous model describes

TABLE III. Quark model parameters appearing in Eqs. (34), (35), and (38).

Quark mass	$m_c$ (MeV)	1763
Confinement	$a_c$ (MeV)	507.4
	$\mu_c$ (fm <sup>-1</sup> )	0.576
	$\Delta$ (MeV)	184.432
OGE	$a_s$	0.81
	$\alpha_0$	2.118
	$\Lambda_0$ (fm <sup>-1</sup> )	0.113
	$\mu_0$ (MeV)	36.976
	$\hat{r}_0$ (fm)	0.181
	$\hat{r}_g$ (fm)	0.259

successfully the meson spectroscopy [25] and provides a good agreement with the experimental data of different physical observables as the strong and radiative decays of charmonium performed in Ref. [38].

As we have discussed above it is interesting to inquire about the real need of form factors which, while providing an acceptable phenomenology, are introduced *ad hoc* to avoid the short-distance divergences. Indeed, if the short-distance regulators are removed, i.e.  $r_0, r_g \rightarrow 0$ , the expressions of our potentials become Eq. (19) for the OGE piece and the confinement part remains the same as in Eq. (35) as this latter contribution does not depend on regulators. We will use these expressions for the potentials in the renormalization scheme. Note that we have also discarded the Dirac delta functions. While this may seem weird, these are distributions which are not seen in the compact support test functions implicitly implied by the boundary condition regularization. This also applies to any derivatives of the Dirac delta function. This result was suggested [27] and explicitly checked by using a momentum space regularization with so-called counter-terms [33].

Moreover, the form factors are naturally adjusted in order to reproduce some well-established physical observables, such as the  $J/\psi$  mass and its leptonic width. What will be shown below is that one can actually treat these observables as suitable renormalization conditions, without any specific need of form factor regulators.

## V. RENORMALIZED CHARMONIUM MODEL

### A. Masses (uncoupled case)

In this section we carry out the renormalization, presented previously along the lines described in detail in Sec. II, for the unregularized model potential. While the tensor force induces a mixing between  $S$  and  $D$ -waves we will in a first step neglect such a mixing. This implies that both ground states are completely unrelated and renormalization is pursued independently. As expected, the charmonium masses in this scheme depend on the short-distance cutoff,  $r_c$ . Figure 6 shows this dependence for the first radial excitations of  $S$  and  $D$ -wave charmonium states. One can see that at some value of  $r_c$  the masses do not depend on the short-distance cutoff.

In Table IV the masses predicted by the renormalized charmonium model and the standard constituent quark model (with form factors) are displayed. We find a perfect agreement between both schemes. This provides confidence on the way the original model took into account the unknown short-distance dynamics, on the one hand, and also on the irrelevance of those form factors for excited states as long as the ground state mass is fixed.

As it becomes clear from the expressions of the potential, the perturbative and nonperturbative contributions

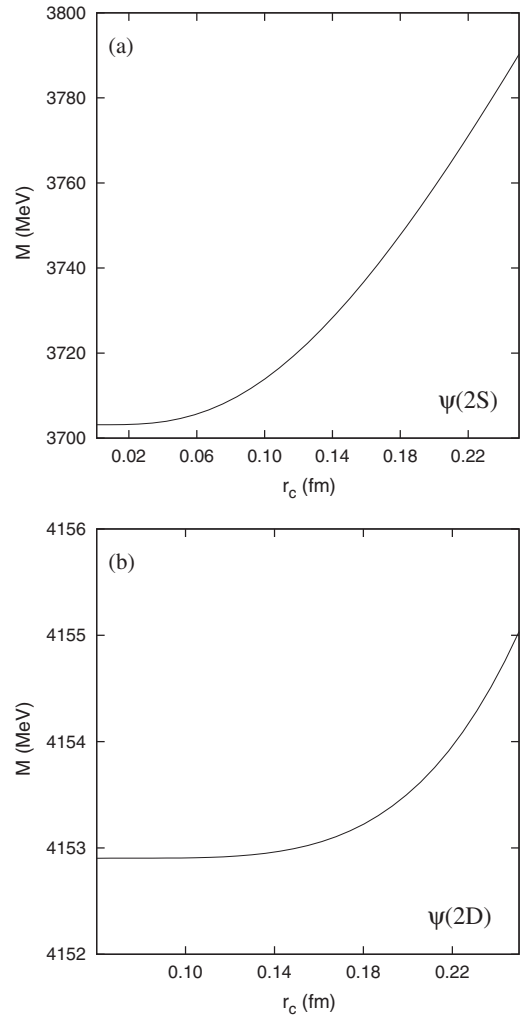


FIG. 6. Dependence of the mass (in MeV)  $2^3S_1$  (upper panel) and  $2^3D_1$  (lower panel) excited charmonium states on the short-distance cutoff,  $r_c$  (in fm).

dominate at short and large distances, respectively. Therefore, we want to study now the dependence of the mass with respect to two important model parameters, the strong coupling constant,  $\alpha_s$ , and our effective string

TABLE IV. Predicted charmonium masses (in MeV) within the renormalization scheme (RSC) and potential model with form factors (CQM). We take  $M_{J/\psi} = 3096.916$  MeV as input.

State	n	$M_{\text{RSC}}$ (MeV)	$M_{\text{CQM}}$ (MeV)	$M_{\text{exp}}$ (MeV)	Ref.
$3S_1$	1	input	3096	$3096.916 \pm 0.011$	[39]
	2	3703	3703	$3686.093 \pm 0.034$	[39]
	3	4097	4097	$4039.6 \pm 4.3$	[39]
	4	4389	4389	$4361 \pm 9 \pm 9$	[40]
	5	4614	4614	$4634_{-7-8}^{+8+5}$	[41]
$3D_1$	1	3796	3796	$3772.92 \pm 0.35$	[39]
	2	4153	4153	$4153 \pm 3$	[39]
	3	4426	4426	$4421 \pm 4$	[39]
	4	4641	4641	$4664 \pm 11 \pm 5$	[40]

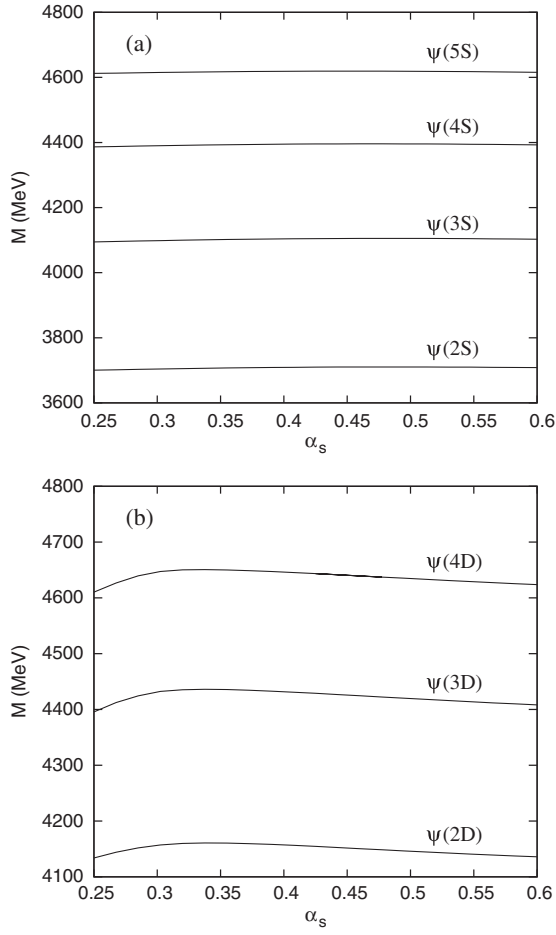


FIG. 7. Mass (in MeV) dependence on the strong coupling constant of excited charmonium states.

tension of the confinement potential,  $\sigma$ , featuring those short and long distance effects.

The dependence on  $\alpha_s$  while fixing the threshold for confinement,  $V_{\text{thr}}$  in Eq. (37), can be seen in Fig. 7 for  $S$  and  $D$ -wave states. For  $S$ -wave states the mass changes about 15 MeV meaning a 0.4% change in the total mass and we see a flattening behavior along the considered range of  $\alpha_s$ . We find a similar trend for the  $D$ -wave states, although in this case the change in mass is larger than in the case of  $S$ -wave states, the picture shows again a rather clear plateau.

We now turn to the mass dependence on the effective string tension of our confinement potential. Again and for clarity of presentation we fix the threshold for confinement,  $V_{\text{thr}}$  in Eq. (37). Figure 8 shows such a dependence for the  $S$  and  $D$ -wave states. The range for the effective string tension is in percentage level equal than the range of the strong coupling constant and we can see that the masses change on the hundreds of MeV. We can conclude that at least the masses of excited states are dominated by the confinement potential as long as the ground state mass is kept to its physical value. In

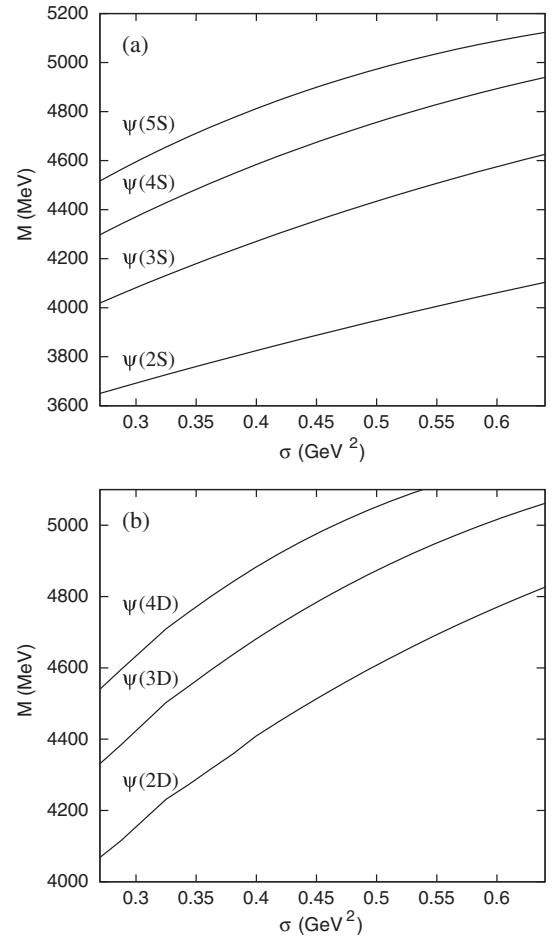


FIG. 8. Dependence of the mass (in MeV) excited charmonium states on the effective string tension of our confinement potential,  $\sigma = -a_c \mu_c (\vec{\lambda}_i^c \cdot \vec{\lambda}_j^c)$  (in  $\text{GeV}^2$ ).

Appendix D we further analyze the sensitivity of the renormalized model parameters.

## B. Leptonic widths

We now focus on the leptonic widths. This will illustrate the interesting subject of the wave function renormalization. A complete calculation of  $V(\text{vector meson}) \rightarrow e^+ e^-$  widths involves radiative and relativistic contributions. The leptonic decay for  $S$ -wave states is given by [42]

$$\Gamma(n^3S_1 \rightarrow e^+ e^-) = \frac{4\alpha^2 e_c^2 |R_{nS}(0)|^2}{M_n^2} \left(1 - \frac{16\alpha_s}{3\pi}\right), \quad (39)$$

where  $e_c = 2/3$  and  $M_n$  is the mass of the charmonium state. Decay widths depend on the value of the wave function at short distances. Of course while the decay may be triggered by a short-distance operator, we may predict decay *ratios* as

$$\mathcal{R} = \frac{\Gamma(n^3S_1 \rightarrow e^+ e^-)}{\Gamma(1^3S_1 \rightarrow e^+ e^-)} = \frac{|R_{nS}(0)|^2 M_1^2}{|R_{1S}(0)|^2 M_n^2}. \quad (40)$$

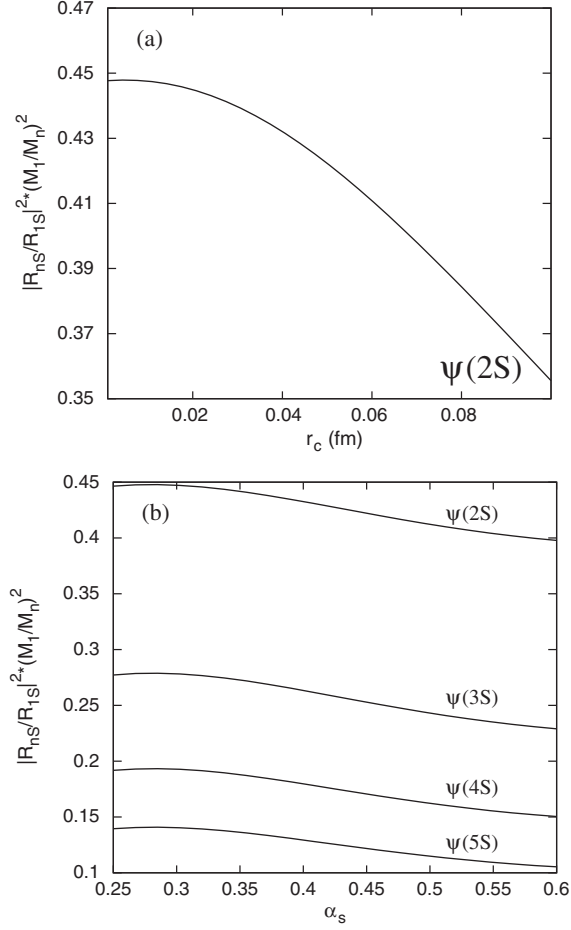


FIG. 9. Top picture shows the dependence of the ratio  $\mathcal{R}$  with respect to short-distance cutoff,  $r_c$ . Bottom picture shows the dependence of the ratio  $\mathcal{R}$  for the excited  $S$ -wave charmonium states on the strong coupling constant,  $\alpha_s$ .

This corresponds in practice to implement a common wave function renormalization which factors out in the ratio.

Figure 9(a) shows the dependence of  $\mathcal{R}$  with respect to the short-distance cutoff for the first radial excitation of  $S$ -wave states. At some range of  $r_c$ , the ratio does not depend on its value. Figure 9(b) shows the dependence of

the ratio for the  $S$ -wave states along the range of strong coupling constant. This range is the same as in the case of studying masses. We find a stronger dependence on the strong coupling constant as expected since the leptonic decay is a short range observable.

### C. Gluonic and photonic widths

It is straightforward to extend the previous analysis to the  $\psi(nS) \rightarrow 3g$  and  $\psi(nS) \rightarrow 3\gamma$  cases. So the corresponding formulas are [43]

$$\Gamma(n^3S_1 \rightarrow 3g) = \frac{40(\pi^2 - 9)\alpha_s^3 |R_{nS}(0)|^2}{81\pi M_n^2} \left[ 1 - 3.7 \left( \frac{\alpha_s}{\pi} \right) \right], \quad (41)$$

$$\Gamma(n^3S_1 \rightarrow 3\gamma) = \frac{16(\pi^2 - 9)\alpha_s^6 |R_{nS}(0)|^2}{3\pi M_n^2} \left[ 1 - 12.6 \left( \frac{\alpha_s}{\pi} \right) \right]. \quad (42)$$

Clearly we see that the ratios from excited states to the ground state are process independent and identical to the corresponding leptonic decay widths discussed above

$$\frac{\Gamma(n^3S_1 \rightarrow 3g)}{\Gamma(1^3S_1 \rightarrow 3g)} = \frac{\Gamma(n^3S_1 \rightarrow 3\gamma)}{\Gamma(1^3S_1 \rightarrow 3\gamma)} = \frac{\Gamma(n^3S_1 \rightarrow e^+e^-)}{\Gamma(1^3S_1 \rightarrow e^+e^-)}. \quad (43)$$

This obviously allows to predict the excited states decay widths from the experimental ground state decay widths. The results are presented in Table V.

### D. Inclusion of coupled channels

Finally, we take into account the role played by the tensor force which, as we know from previous sections, is responsible for the mixing between  $S$  and  $D$ -waves in the case of charmonium. The interesting aspect of applying the renormalization procedure to  $S - D$  coupled case is that using just one renormalization condition, the mass of the  $J/\psi$ , we can predict all  $S$  and  $D$ -wave mesons.

TABLE V. Absolute decay widths for excited charmonium states. We use the ground state experimental width as input. The quoted errors reflect the uncertainty stemming from the ground state only.

$\psi(nS)$	$\psi(nS) \rightarrow e^+e^-$		$\psi(nS) \rightarrow 3g$		$\psi(nS) \rightarrow 3\gamma$	
	$\Gamma_{\text{The}}$ (keV)	$\Gamma_{\text{Exp}}$ (keV)	$\Gamma_{\text{The}}$ (keV)	$\Gamma_{\text{Exp}}$ (keV)	$\Gamma_{\text{The}}$ (eV)	$\Gamma_{\text{Exp}}$ (eV)
1S	input	$5.55 \pm 0.14$	input	$59.5 \pm 2.0$	input	$1.11 \pm 0.37$
2S	$2.49 \pm 0.06$	$2.33 \pm 0.07$	$26.7 \pm 0.9$	$30.3 \pm 4.9$	$0.49 \pm 0.18$	-
3S	$1.55 \pm 0.04$	$0.86 \pm 0.07$	$16.6 \pm 0.6$	-	$0.31 \pm 0.11$	-
4S	$1.08 \pm 0.03$	-	$11.5 \pm 0.4$	-	$0.21 \pm 0.08$	-
5S	$0.78 \pm 0.02$	-	$8.4 \pm 0.3$	-	$0.16 \pm 0.06$	-

TABLE VI. Masses (in MeV), the asymptotic  $D/S$  ratio parameter and  $D$ -wave probabilities of charmonium states including  $S$ - $D$  mixture. We take the ground state of the original model  $M_{J/\Psi} = 3096$  MeV as input.

State	M (MeV)	$\eta$	$\mathcal{P}_D$ (%)
$J/\psi$	input	-0.012	0.15
$\psi(2S)$	3703	+0.011	0.22
$\psi(1D)$	3796	-12.5	99.9
$\psi(3S)$	4098	+0.032	0.45
$\psi(2D)$	4152	-9.5	99.6
$\psi(4S)$	4389	+0.052	0.76
$\psi(3D)$	44.25	-7.8	99.3
$\psi(5S)$	4614	+0.070	1.1
$\psi(4D)$	4640	-6.7	98.9

The procedure is the same than in Sec. III with only one difference, where our confining interaction is given by Eq. (35), which flattens out at large distances. So in this case the asymptotic boundary conditions become

$$u(r) \rightarrow A_S e^{-\kappa r}, \quad w(r) \rightarrow A_D \left(1 + \frac{3}{\kappa r} + \frac{3}{(\kappa r)^2}\right) e^{-\kappa r}, \quad (44)$$

with  $\kappa^2 = m_c(V_{\text{thr}} + 2m_c - M)$  and  $V_{\text{thr}}$  given by Eq. (37).

Results on the mass, the asymptotic  $D/S$  ratio parameter, and  $D$ -wave probability are presented in Table VI. The comparison between renormalization scheme and constituent quark model with form factors is given in Table VII. One can see that the agreement is completely satisfactory. Essentially, this proves that the form factors only provide the correct mass of  $J/\psi$ . Once this is fixed the rest of the excited states with either  $S$ - or  $D$ - wave character are predicted. This is the main result of the present study.

## VI. ON THE APPLICABILITY OF THE RENORMALIZATION PROCEDURE

In most examples shown in this paper, we have always dealt with a situation where it was possible to fix the energy of a bound state, so that there is a mild dependence of excited states on the short-distance cutoff. This scaling analysis is carried out in Appendix A providing an understanding of the features found numerically.

Of course, there is the question when the present renormalization procedure is guaranteed to work, i.e. can we always mock up our ignorance at short distances by a given renormalization condition? On the other hand it is also important to know if the answer is affirmative what does the renormalization tell about the true solution?

### A. Renormalization of the bosonic-string potential

It is instructive to analyze first the case where renormalization can be carried out at any level of approximation of the “true” potential. We provide some insight into the renormalization problem by analyzing in some detail the bosonic string model (BSM) [30,31]. Such a model provides an alternative approach to the physics of confinement from the point of view of large distances (for a review see e.g. [44]). It should be noted that with the constraint  $\alpha_s = \pi/16$ , the Cornell potential corresponds to the large-distance expansion of the following potential:

$$V(r) = \sigma \sqrt{r^2 - r_0^2} = \sigma r - \frac{\sigma r_0^2}{2r} - \frac{\sigma r_0^4}{8r^3} + \dots, \quad (45)$$

where  $\sigma r_0^2 = \pi/6$ . With the standard value for the string tension  $\sqrt{\sigma} = 0.420$  GeV one has  $r_0 \sim 0.3$  fm. A feature of this potential is that for  $r < r_0$  it becomes purely imaginary. Moreover, lattice calculations [29] yield  $4\alpha_s/3 = 0.25(1)$ , extremely close to the BSM choice of  $\alpha_s = \pi/16$  when the Cornell potential,

TABLE VII. Comparison of different properties of charmonium between the renormalization scheme and the constituent quark model with form factors, considering coupled channels in both cases. We take  $M_{J/\Psi} = 3096$  MeV as input.

Meson	n	Renormalized scheme			Form factors scheme			Exp. data
		$\mathcal{P}_{3S_1}$ (%)	$\mathcal{P}_{3D_1}$ (%)	$M$ (MeV)	$\mathcal{P}_{3S_1}$ (%)	$\mathcal{P}_{3D_1}$ (%)	$M$ (MeV)	
$J/\psi$	1	99.85	0.15	input	99.96	0.04	3096	$3096.916 \pm 0.011$
$\psi(2S)$	2	99.78	0.22	3703	99.96	0.04	3703	$3686.093 \pm 0.034$
$\psi(3770)$	3	0.15	99.85	3796	0.03	99.97	3796	$3772.92 \pm 0.35$
$\psi(4040)$	4	99.55	0.45	4098	99.94	0.06	4097	$4039.6 \pm 4.3$
$\psi(4160)$	5	0.39	99.61	4152	0.06	99.94	4153	$4153 \pm 3$
$X(4360)$	6	99.24	0.76	4389	99.91	0.09	4389	$4361 \pm 9 \pm 9$
$\psi(4415)$	7	0.72	99.28	4426	0.09	99.91	4426	$4421 \pm 4$
$X(4630)$	8	98.89	1.11	4614	99.88	0.12	4614	$4634^{+8}_{-7-8}$
$X(4660)$	9	1.08	98.92	4640	0.11	99.89	4641	$4664 \pm 11 \pm 5$

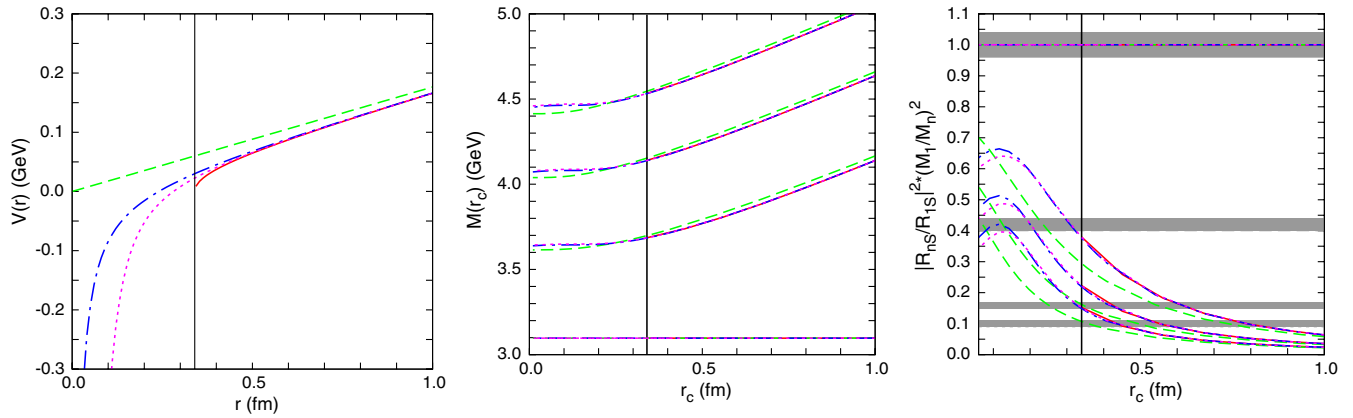


FIG. 10 (color online). *Left panel:* The bosonic-string model potential (in GeV) and different terms contributing to the long-distance expansion truncated to a given order as a function of the distance  $r$  (in fm). *Middle panel:* Short-distance cutoff  $r_c$  (in fm) dependence of the  $S$ -wave charmonium spectrum masses (in GeV) for the different approximations to the potential. *Right panel:* Relative  $n^3S_1 \rightarrow e^+e^-$  decay ratios with respect the leptonic width of the ground state,  $J/\psi \rightarrow e^+e^-$ . The bands indicate the corresponding experimental number. In all cases the vertical line marks the critical radius below which the full potential becomes imaginary. Solid line: Full BSM. Dashed line: LO approximation. Dashed-dotted: NLO. Dotted line: NNLO.

Eq. (3), is taken. It has been found [45] that the transition from perturbative to string behavior is evident from the data and takes place at surprisingly small distances.<sup>7</sup>

The BSM potential satisfies exact fundamental inequalities for the Wilson loop exploiting reflection positivity [16,17], namely,

$$V'(r) > 0 \quad V''(r) \leq 0. \quad (46)$$

The latter identity is saturated by the linear potential. This is satisfied by *any* inverse power series with negative coefficients, i.e.

$$V(r) = \sigma r + V_0 + \sum_{n=1}^{\infty} c_n/r^n, \quad (47)$$

where one has  $c_n \leq 0$ . However, note that the converse need not be true, namely, Eq. (46) does not necessarily imply that *all* coefficients in Eq. (47) are negative.

In this section we deal with the renormalization of the bosonic-string potential given by Eq. (45). Of course, this potential is questionable below the critical radius where it becomes imaginary. On the other hand, if the large-distance expansion is truncated to a finite order we have to deal with increasingly singular power divergences. We will illustrate how the renormalization procedure works when the full potential is compared to the series of singular potentials at the origin.

<sup>7</sup>This of course raises the question on whether the perturbative OGE contribution,  $-4\alpha_s(\mu)/3r$ , should be added on top of the BSM- $1/r$  result or it is actually dual to it, in which case a scale of  $\mu = 2$  GeV is implied, if one demands  $\alpha_s(\mu) = \pi/16$  at LO in perturbation theory.

This example also shows how to treat singular potentials. Indeed, at NNLO one encounters a  $1/r^3$  short-distance divergence. The problem with such a singularity is that the energy becomes unbound from below. To overcome this situation one can fix, as was discussed in Sec. II, the ground state energy and then, using the orthogonality condition, the excited states can be predicted. Of course, this procedure can also be carried out without a singular potential, but just on the basis that the short-distance behavior of the potential may not be fully reliable.

Our numerical results are displayed in Fig. 10. There we show the BSM potential compared to the linear  $V_{\text{LO}}(r) = \sigma r$  (LO),  $V_{\text{NLO}}(r) = \sigma r + c_1/r$  (NLO) as well as  $V_{\text{NNLO}}(r) = \sigma r + c_1/r + c_3/r^3$  (NNLO) approximations. Actually, for the typical value of the string tension the difference between the potentials is at most about 50 MeV. Applying the renormalization procedure we see that when the short-distance cutoff coincides with the critical distance the difference among the different masses become much smaller. This is just a manifestation of the short-distance insensitivity embodied by the renormalization. While in the exact BSM we are forced to stop at the critical radius, the LO, NLO, NNLO, ... truncations to such a potential allow to remove the cutoff completely. However, as we see from the figure this provides in our view an estimate on the systematic error inherent to the BSM model; the mass shift generated by the different truncations is about 50 MeV. Of course, there is no point in going beyond such an accuracy before other important effects (like e.g. relativistic corrections) are taken into account.

Actually, there are hints [46,47] that for the Nambu-Goto string the critical radius moves about a factor of two down (in our case it means  $\sim 0.2$  fm) when quark masses

become comparable to the string tension  $m_q/\sqrt{\sigma} \sim 1$  (in our case  $m_c/\sqrt{\sigma} = 2.85$ ).<sup>8</sup>

We depict the relative  $n^3S_1 \rightarrow e^+e^-$  decay ratios with respect to the ground state  $J/\psi \rightarrow e^+e^-$  decay. As we have emphasized above the advantage of such a comparison is that purely perturbative and state independent corrections in the van Royen-Weisskopf formula are factorized out. However, note that the very use of this formula assumes a regular potential. Thus we take naturally the wave function at the shortest cutoff radius,  $r_c$ . As we can see there are somewhat large differences for the simple linear potential (LO) approximation as compared to NLO, NNLO or the full BSM results which agree among them, displaying a convergent pattern at any value of  $r_c$ . Differences between NLO and NNLO start being noticeable below the cutoff radius of about 0.15 fm for the first excited state, although the value seems slightly displaced to larger numbers for the next excited states, as one might expect from their stronger short-distance sensitivity. Also interesting is the fully converged result at  $r_c \rightarrow 0$ , a fact which follows analytically by a detailed study of the short-distance wave functions (see Appendix C).

These features reinforce the value of renormalization as a way to study the effect of improving on the long-distance components of the  $\bar{q}q$  potential. Indeed, even though the NNLO potential strongly diverges at short distances the effects on the short-distance wave function are not out of control; the relevant scale is provided by the binding energy of the bound state.

Of course, while the outgoing decay ratios seem to reproduce the experimental numbers above the critical radius, it is not completely obvious whether fixing the short-distance cutoff radius is fully justified, as the decay formula corresponds to the strict infinite mass and point-like limit of the related electromagnetic matrix element  $\gamma \rightarrow q\bar{q}$ . Actually, the momentum dependence and recoil effects due to the incoming virtual photon have been dealt with in Ref. [49] where the corresponding modification to the standard decay formula decreases its value substan-

<sup>8</sup>We also note a recent effective string theory approach [48], where these finite mass effects are evaluated regardless on the specific string dynamics, yielding a potential, up to a constant term, of the form

$$V(r) = \frac{1}{m} \left[ \frac{g^2 \Lambda^4}{\pi \kappa} \log(\sqrt{\kappa} r) \right], \quad (48)$$

hence they obtain the nontrivial result that the  $1/m$  potential must grow logarithmically at large  $r$  and it has to connect with the  $1/r^2$  behavior at short distances of the  $1/m$  contribution calculated by perturbation theory. The comparison of the lattice data is done through the next potential form

$$V_{\text{fit}}(r) = \frac{1}{m} \left[ \frac{-c'}{r^2} + d' \ln\left(\frac{r}{r_0}\right) \right], \quad (49)$$

where once a fit to the lattice data is done [20,21] yields  $c' = 0.0027 \text{ GeV}^2$  and  $d' = 0.0075 \text{ GeV}^2$ .

TABLE VIII. Relative  $n^3S_1 \rightarrow e^+e^-$  decay ratios with respect to the ground state  $J/\psi \rightarrow e^+e^-$  decay calculated through the van Royen-Weisskopf formula and taking into account momentum dependence and recoil effects according to Ref. [49].

State	$\mathcal{R}_{\text{Weisskopf}}$	$\mathcal{R}_{\text{Leinweber}}$
$J/\psi$	1.00	1.00
$\psi(2S)$	0.58	0.58
$\psi(3S)$	0.41	0.42
$\psi(4S)$	0.31	0.32

tially. In Appendix B we collect some relevant formulas. In our case we see that, as expected, there is an increasing suppression for excited states, although in the ratio this effect is negligible as can be seen from Table VIII.

In summary, the analysis shows that even if one can apply the renormalization to any long-distance approximation to the BSM potential, due to the existence of the scale  $r_0$ , one should not take  $r_c \rightarrow 0$ , but rather to keep  $r_c \sim r_0$  to comply with the dynamics.

## B. Singular repulsive interactions

To analyze a situation where renormalization conditions cannot be applied let us consider the case where in the power series expansion Eq. (47) one term happened to be singular and repulsive at short distances, say for  $n = 3$  (unlike the BSM discussed above). Then the solution would be of the form

$$u(r) \rightarrow r^{3/4} [C_{1R} e^{2(R/r)^{1/2}} + C_{2R} e^{-2(R/r)^{1/2}}], \quad (50)$$

where we have a converging and a diverging exponential at the origin.

Clearly, if we impose normalizability of the bound state, the regular solution must be chosen. In such a case the bound state energy is *predicted* as it usually happens for the standard nonsingular quantum mechanical potentials. Conversely, if the bound state energy is chosen *arbitrarily* then the wave function is non-normalizable at short distances. In this sense, the rigorous results given by Eq. (46), valid in the infinite mass limit, which imply that *all* inverse powers are attractive singularities, are most welcome, because this would imply that the problem of a repulsive singularity of a *truncated* potential is related to the truncation itself. As we have mentioned, these violations of the conditions featured by Eq. (46) are also observed in perturbation theory (see e.g. [15]).

Finally, it is not obvious what might be the situation for relativistic corrections which on purely dimensional grounds are of the general form

$$V(r) \sim \frac{1}{m^n} \frac{p^k}{r^{k+n+1}}. \quad (51)$$

Of course, Weyl ordering should be applied to make sure that the operator is Hermitian [50]. However, as shown in

[51,52] one can eliminate the  $p$  dependence in terms of  $L$  dependence at the expense of reshuffling the  $1/m$  expansion. Ultimately, we end up with singular problems which generally depend on the angular momentum, showing that one must possibly use a different renormalization condition for each partial wave. However, note that for this to happen one must have a singular attractive singularity. This interesting topic deserves further investigation.

## VII. CONCLUSIONS

We have reanalyzed the calculation of the  $1^{--}$  charmonium spectrum in a constituent quark model using a renormalization boundary condition scheme. This approach avoids explicitly the introduction of phenomenological form factors used in the past which are usually fine-tuned to low-lying mesonic observables. In fact this fine tuning feature is commonplace to many approaches beyond the limited framework of the constituent quark model.

The renormalization viewpoint actually uses these low-lying properties as input parameters and sidesteps the fine-tuning, as illustrated in several examples. For the phenomenologically successful model of Ref. [25] where *ad hoc* form factors are introduced as regulators, we find an almost perfect agreement with the renormalization approach. This result provides confidence on the way the original model took into account the unknown short-distance dynamics. The use of the renormalization scheme allows us to further study the dependence of the states on the model parameters in a cleaner way since the regulator dependence has been removed.

We find that the mass of the excited states strongly depends on the string tension parameter as one would naturally expect. Further, there is also a remarkable insensitivity to the strong coupling constant entering the one-gluon exchange contribution of the potential. This avoids a great deal of unphysical fine-tuning which suggested taking for this parameter unnaturally large values  $\alpha_s = 0.3-0.4$ . In contrast, the leptonic decay widths present a marked dependence on the strong coupling constant, as expected likewise because these are short-range observables.

We also show how the consistency of the renormalization conditions relates the spectrum of  $S$ - and  $D$ -waves of the  $1^{--}$  sector via the OGE tensor force interaction. Amazingly, the  $J/\Psi$  state generates not only the  $S$ -wave dominated states but also the almost pure  $D$ -wave states in a satisfactory manner. This rather intriguing result is genuinely nonperturbative and deserves further study as it suggests a reduction of parameters which might be helpful in the analysis of EFT approaches.

Of course, a more complete description of charmonium systems should also take explicitly into account the contribution to the open charm channels which will provide mass shifts and widths for unstable quark-antiquark bound

states. In summary, the renormalization approach traces quite naturally and explicitly the long- and short-distance dependence of hadronic properties.

## APPENDIX A: RENORMALIZATION CONDITIONS AND ERROR ESTIMATES

The boundary condition allows to connect the bound state to the excited states by the matching condition. We provide here an *a priori* and qualitative determination on the short-distance cutoff error of a excited state,  $E_n(r_c)$  when the ground state is fixed to a given value  $E_0$  for *any value* of the cutoff  $r_c$ .

We start with the ground state energy,  $E_0$ , which is fixed throughout and compute the logarithmic derivative of the ground state wave function at  $r_c$  which is matched to the corresponding quantity of the excited state. Then, we perform a calculation of the bound state energy,  $E_n(r_c)$ , which obviously depends on the cutoff radius. It is this  $r_c$  dependence the one we want to determine. Let us denote by  $u_n(r, r_c)$  the excited wave function where the dependence on  $r_c$  is explicitly displayed. Under an infinitesimal change,  $r_c \rightarrow r_c + \Delta r_c$  we get

$$-\Delta u_n'' + U\Delta u_n = \Delta E_n u_n + E_n \Delta u_n. \quad (\text{A1})$$

Note that the variation is defined for a *fixed* value of  $r$ ,

$$\Delta u_n(r, r_c) = u_n(r, r_c + \Delta r_c) - u_n(r, r_c), \quad (\text{A2})$$

and hence

$$\Delta u_n'(r, r_c) = u_n'(r, r_c + \Delta r_c) - u_n'(r, r_c), \quad (\text{A3})$$

where here, the prime denotes derivative with respect to the  $r$  variable. Therefore, if we use the boundary condition

$$u_n'(r_c, r_c) = L_n(r_c)u_n(r_c, r_c), \quad (\text{A4})$$

we get

$$\Delta u_n'(r, r_c)|_{r=r_c} = \Delta(L_n(r_c)u_n(r_c, r_c)) - \frac{\partial u_n'(r, r_c)}{\partial r_c} \Big|_{r=r_c} \Delta r_c. \quad (\text{A5})$$

From here we obtain

$$(L_n' + L_n^2 - U + E_n)u_n = -\frac{\partial u_n'}{\partial r_c} + L_n \frac{\partial u_n}{\partial r_c}, \quad (\text{A6})$$

and multiplying this equation by  $u_n$  and subtracting the original equation multiplied by  $\Delta u_n$  we get

$$-\Delta u_n'' u_n + u_n'' \Delta u_n = \Delta E_n u_n^2, \quad (\text{A7})$$

which integrating from  $r_c$  and infinity and using that for a bound state  $u_n(r, r_c) \rightarrow 0$  at large distances we get

$$-\Delta u_n' u_n + u_n' \Delta u_n = \Delta E_n \int_{r_c}^{\infty} u_n^2. \quad (\text{A8})$$

On the other hand, since the ground state energy is fixed,  $\Delta E_0 = 0$ , we get



$$-\Delta u'_0 u_0 + u'_0 \Delta u_0 = 0, \quad (\text{A9})$$

and taking into account

$$\Delta E_n = (L'_n + L_n^2 - U + E_n) \frac{u_n(r_c)^2}{\int_{r_c}^{\infty} u_n(r)^2 dr}, \quad (\text{A10})$$

so that using  $L_n = L_0$  we arrive at

$$\Delta(E_n - E_0) = (E_n - E_0) \frac{u_n(r_c)^2}{\int_{r_c}^{\infty} u_n(r)^2 dr} \Delta r_c. \quad (\text{A11})$$

Actually, integrating we get

$$[E_n(r_c) - E_0] \int_{r_c}^{\infty} dr u_n(r)^2 = \text{const}. \quad (\text{A12})$$

For a normalized state we have for small  $r_c$

$$E_n(r_c) - E_0 = (E_n - E_0)[1 + r_c u_n(r_c)^2 + \dots] \quad (\text{A13})$$

Therefore for a regular potential with a nontrivial boundary condition  $u_n(0) \neq 0$  the error is at least linear. For a singular and attractive potential,  $1/r^n$ , the error is  $\mathcal{O}(r_c^{1+n/2})$  up to some oscillations. As we see, the convergence is from above and proportional to the energy difference as well. This means that the effect of putting a finite cutoff fixing the ground state energy is repulsive and increases with the excitation energy.

## APPENDIX B: MOMENTUM DEPENDENCE AND RECOIL EFFECTS AS CORRECTIONS TO LEPTONIC WIDTHS

Momentum-dependent effects could reveal significant corrections to the theoretical leptonic width. The expression for  $e^+e^-$  decay width of  $S$ -wave states in the center-of-mass frame of the meson and taking into account those effects can be written as [49]

$$\begin{aligned} \Gamma(e^+e^-) &= 16\alpha^2 e_q^2 \frac{m_q^2}{M^4} \frac{|\vec{k}|}{E_e} (3E_e^2 - |\vec{k}|^2) \left[ \int_0^{\infty} \frac{E_q + m_q}{m_q} \right. \\ &\quad \left. \times \frac{|\vec{p}|^2}{E_q} \left( 1 + \frac{|\vec{p}|^2}{3(E_q + m_q)^2} \right) \psi(|\vec{p}|) d|\vec{p}| \right]^2, \end{aligned} \quad (\text{B1})$$

where  $e_q$  is the quark charge in units of the charge of the electron,  $M$  is the mass of the meson, and

$$E_q = (|\vec{p}|^2 + m_q^2)^{1/2}, \quad E_e = (|\vec{k}|^2 + m_e^2)^{1/2}, \quad (\text{B2})$$

are the quark and lepton energies, respectively.

The static limit of Eq. (B1) may be obtained by considering the nonrelativistic limit

$$\frac{|\vec{p}|^2}{m_q^2} \ll 1 \quad (\text{B3})$$

and in this case the integral in Eq. (B1) reduces to

$$\frac{2}{m_q} \int_0^{\infty} \psi(|\vec{p}|) |\vec{p}|^2 d|\vec{p}|. \quad (\text{B4})$$

Recalling the Fourier transform

$$\phi(\vec{r}) = \frac{1}{(2\pi)^{3/2}} \int e^{i\vec{p}\cdot\vec{r}} \psi(\vec{p}) d\vec{p} \quad (\text{B5})$$

and evaluating at the origin, we have

$$\begin{aligned} \phi(\vec{r} = 0) &= \frac{1}{(2\pi)^{3/2}} \int \psi(\vec{p}) d\vec{p} \\ &= \sqrt{\frac{2}{\pi}} \int_0^{\infty} |\vec{p}|^2 \psi(|\vec{p}|) d|\vec{p}|, \end{aligned} \quad (\text{B6})$$

so the integral above, Eq. (B4), becomes

$$\frac{2}{m_q} \int_0^{\infty} \psi(|\vec{p}|) |\vec{p}|^2 d|\vec{p}| = \frac{(2\pi)^{1/2}}{m_q} |\phi(\vec{r} = 0)|^2. \quad (\text{B7})$$

With the kinematic relationships, the static limit of Eq. (B1) is

$$\Gamma(e^+e^-)|_{\text{static}} = \frac{16\pi\alpha^2 Q^2}{M^2} |\phi(\vec{r} = 0)|^2, \quad (\text{B8})$$

which is the well-known van Royen-Weisskopf formula.

Figure 11 shows the comparison of the relative  $n^3S_1 \rightarrow e^+e^-$  decay ratios with respect the leptonic width of the ground state,  $J/\psi \rightarrow e^+e^-$ . The ratios are calculated by van Royen-Weisskopf and Leinweber formulas. Left, middle, and right panels of the figure show the results for the different terms contributing to the long-distance expansion of the bosonic-string model truncated to a given order (LO, NLO, and NNLO).

## APPENDIX C: SHORT-DISTANCE ANALYSIS OF WAVE FUNCTIONS

### 1. Single channel case

In this appendix we summarize a few interesting facts concerning the short-distance behavior of wave functions. In the OGE case an attractive Coulomb like behavior holds, so that at short distances the reduced potential reads

$$U(r) \equiv 2\mu V(r) \rightarrow -\frac{1}{Rr}, \quad (\text{C1})$$

$R$  represents the relevant length scale in the reduced potential. Thus for the  $nS$  state we have short-distance behavior

$$u_n(r) \rightarrow A_n \left[ 1 - \frac{3r}{2R} - \frac{r}{R} \log\left(\frac{r}{R}\right) \right] + B_n r, \quad (\text{C2})$$

which is a linear combination of the regular wave function and the singular one. Note that since the ground state has a given energy the irregular component does not vanish. On the other hand, the orthogonality condition, Eq. (7), implies  $A_n/B_n = A_0/B_0$  so that

$$\frac{u_n(r_c)}{u_0(r_c)} \rightarrow \frac{A_n}{A_0}, \quad (\text{C3})$$

which shows that the ratio between wave functions becomes finite as the cutoff is removed, as can be seen at the right panel in Fig. 10.

For a power-like short-distance singular potential we may keep the strongest singularity

$$V(r) \rightarrow -\frac{C_n}{r^n}. \quad (\text{C4})$$

The solution of the Schrödinger equation requires the reduced potential

$$U(r) \equiv 2\mu V(r) \rightarrow -\frac{1}{R^2} \left(\frac{R}{r}\right)^n, \quad (\text{C5})$$

where for convenience the variable  $R = (2\mu C_n)^{1/4}$  with length scale dimensions has been introduced. At short distances the reduced de Broglie wavelength is given by

$$\lambda(r) \equiv \frac{1}{\sqrt{-U(r)}} = R \left(\frac{r}{R}\right)^{n/2}, \quad (\text{C6})$$

which fulfills

$$\frac{d\lambda(r)}{dr} = \frac{n}{2} \left(\frac{r}{R}\right)^{(n/2)-1} \ll 1, \quad (\text{C7})$$

for  $r \ll R$ . In such a case the WKB method can be applied [53] yielding

$$u(r) \rightarrow u_{\text{WKB}}(r) = \frac{A}{[-U(r)]^{1/4}} \sin \left[ \int dr \sqrt{-U(r)} + \varphi \right], \quad (\text{C8})$$

where  $A$  and  $\varphi$  are undetermined amplitude and phase which may be obtained by matching to the exact solution in the region  $r \sim R$ . In the case of the singular potential given by Eq. (C4) we have for the  $m$ -state

$$u_m(r) \rightarrow A_m \left(\frac{r}{R}\right)^{n/4} \sin \left[ \frac{2}{2-n} \left(\frac{R}{r}\right)^{(n/2)-1} + \varphi_m \right]. \quad (\text{C9})$$

However, the orthogonality condition, Eq. (7), imply  $\varphi_m = \varphi_0$ . Thus we obtain

$$\frac{u_m(r_c)}{u_0(r_c)} \rightarrow \frac{A_m}{A_0}, \quad (\text{C10})$$

which shows that the ratio between wave functions becomes finite as the cutoff is removed. For  $n = 3$  this is seen at the right panel in Fig. 10.

## 2. Coupled channel case

Here we undertake the short-distance analysis of the spin-orbit and tensor interactions. At short distances one may neglect all terms and just keep the  $1/r^3$  singular contribution yielding

$$\begin{pmatrix} -u''(r) \\ -w''(r) \end{pmatrix} + \frac{R}{r^3} \begin{pmatrix} 0 & \frac{2\sqrt{2}}{3} \\ \frac{2\sqrt{2}}{3} & -\frac{20}{3} \end{pmatrix} \begin{pmatrix} u(r) \\ w(r) \end{pmatrix} = 0. \quad (\text{C11})$$

This system can be diagonalized by going to the rotated basis

$$\begin{pmatrix} v_1(r) \\ v_2(r) \end{pmatrix} = \begin{pmatrix} \cos\alpha & \sin\alpha \\ -\sin\alpha & \cos\alpha \end{pmatrix} \begin{pmatrix} u(r) \\ w(r) \end{pmatrix}, \quad (\text{C12})$$

where the new functions satisfy

$$-v_1''(r) + \frac{R_1}{r^3} v_1(r) = 0, \quad -v_2''(r) - \frac{R_2}{r^3} v_2(r) = 0, \quad (\text{C13})$$

and the  $R_1$  and  $-R_2$  are the corresponding eigenvalues

$$\frac{R_1}{R} = -\frac{10}{3} + 2\sqrt{3} > 0, \quad -\frac{R_2}{R} = -\frac{10}{3} - 2\sqrt{3} < 0, \quad (\text{C14})$$

and the mixing angle is  $\alpha = 1.1^0$ , a rather small value. At short distances the solutions of Eq. (C13) could be analyzed via the WKB method as we have done in the previous section, but for this case we can undertake the analysis in terms of Bessel functions, whose short distance is analytically known. Actually, the solutions of  $-y''(x) - y(x)/x^3 = 0$  are

$$\begin{aligned} \sqrt{x}J_1(2/\sqrt{x}) &= -\frac{x^{3/4}}{\sqrt{\pi}} \cos(\pi/4 + 2/\sqrt{x}) + \dots, \\ \sqrt{x}Y_1(2/\sqrt{x}) &= -\frac{x^{3/4}}{\sqrt{\pi}} \cos(\pi/4 - 2/\sqrt{x}) + \dots, \end{aligned} \quad (\text{C15})$$

whereas the solutions of  $-y''(x) + y(x)/x^3 = 0$  are

$$\begin{aligned} \sqrt{x}K_1(2/\sqrt{x}) &= \frac{1}{2} \sqrt{\pi} x^{3/4} e^{-2/\sqrt{x}} + \dots, \\ \sqrt{x}I_1(2/\sqrt{x}) &= \frac{1}{2\sqrt{\pi}} x^{3/4} e^{2/\sqrt{x}} + \dots, \end{aligned} \quad (\text{C16})$$

All this amounts to write the solutions in the suitable form

$$\begin{aligned} v_1(r) &\rightarrow \left(\frac{r}{R_1}\right)^{3/4} [C_{1R} e^{+2\sqrt{R_1}/r} + C_{2R} e^{-2\sqrt{R_1}/r}], \\ v_2(r) &\rightarrow C_A \left(\frac{r}{R_2}\right)^{3/4} \sin \left[ 2\sqrt{\frac{R_2}{r}} + \varphi \right]. \end{aligned} \quad (\text{C17})$$

The four constants appearing here,  $C_{1R}$ ,  $C_{2R}$ ,  $C_A$ , and  $\varphi$  reflect that the total order of the system is four. The last equation also shows that generally solutions will diverge as  $e^{2\sqrt{R_1}/r}$  at the origin, hence preventing the bound state normalization condition, unless  $C_{1R} = 0$ . In such a case the normalizable solution may be written as

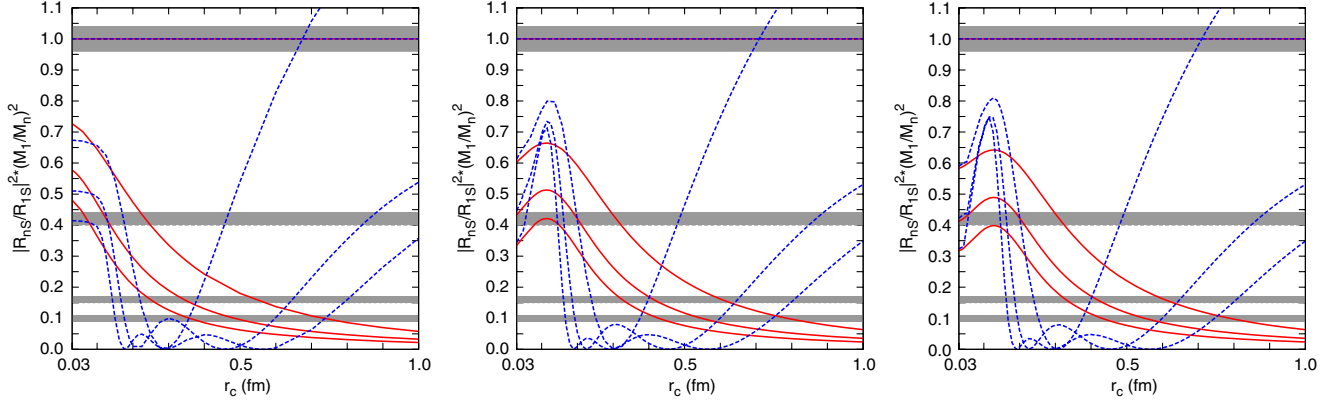


FIG. 11 (color online). Relative  $n^3S_1 \rightarrow e^+e^-$  decay ratios with respect the leptonic width of the ground state,  $J/\psi \rightarrow e^+e^-$  which are calculated by van Royen-Weisskopf (solid line) and Leinweber (dashed line) formulas. *Left panel*: LO. *Middle panel*: NLO. *Right panel*: NNLO.

$$\begin{aligned}
 u(r) &\rightarrow -\sin\alpha C_A \left(\frac{r}{R_2}\right)^{3/4} \sin\left[2\sqrt{\frac{R_2}{r}} + \varphi\right] \\
 &\quad + \cos\alpha C_{2R} \left(\frac{r}{R_1}\right)^{3/4} e^{-2\sqrt{R_1/r}}, \\
 w(r) &\rightarrow \cos\alpha C_A \left(\frac{r}{R_2}\right)^{3/4} \sin\left[2\sqrt{\frac{R_2}{r}} + \varphi\right] \\
 &\quad + \sin\alpha C_{2R} \left(\frac{r}{R_1}\right)^{3/4} e^{-2\sqrt{R_1/r}}. \quad (C18)
 \end{aligned}$$

The three independent constants appearing here for the regular solution  $C_A$ ,  $C_{2R}$ , and  $\varphi$  correspond to fix the energy  $M_{J/\psi}$ , the asymptotic  $D/S$  ratio  $\eta$ , and the normalization condition. Note that when integrating from large distances to short distances with a given bound state energy and an arbitrary  $\eta$  we would always have a contribution from the exponentially diverging solution since  $C_{1R} \neq 0$ . Thus, the condition  $C_{1R} = 0$  predicts  $\eta$  from the bound state energy. The foregoing analysis shows that for the  $1/r^3$  singularity appearing here the solution is ambiguous and the bound state energy for a given state has to be treated as an *input*. Of course, the orthogonality requirement between different states implies that if one state,  $(u_n, w_n)$ , has a short-distance phase  $\varphi_n$  and another state,  $(u_m, w_m)$ , has a short-distance phase  $\varphi_m$ , one has

$$\begin{aligned}
 0 &= 2\mu(M_n - M_m) \int_0^\infty dr (u_n u_m + w_n w_m) \\
 &= [u'_n u_m - u_n u'_m + w'_n w_m - w_n w'_m]_0^\infty \\
 &= \frac{1}{R_2} C_{A,n} C_{A,m} \sin(\varphi_n - \varphi_m) \quad (C19)
 \end{aligned}$$

whence  $\varphi_n = \varphi_m$  is obtained. This shows that all states are linked through the spin-dependent splitting provided the ground state energy is given.

#### APPENDIX D: FITTING PARAMETERS OF THE RENORMALIZED MODEL

It is interesting to see what is the renormalized model sensitivity to the parameters. Of course, at this level one should envisage the possibly non-negligible contribution of the missing mesonic thresholds and the induced mass shift. To this end we fit the model parameters from the experimental masses of  $1^{--} c\bar{c}$  states [39] and estimate their theoretical uncertainties as well as an educated mass-shift guess. The way to perform the first task is of course debatable. This requires some compromise as to what are the errors attached to the masses within the present framework. Naively one would just take the quoted PDG errors on the experimental masses. However, as we have mentioned above, the present model incorporates thresholds but no explicit coupling to meson-meson channels. This affects more significantly the higher excited states via a subthreshold induced mass shift, which we take as a systematic error of the model.

We decide to make a  $\chi^2$  fit using as fitting parameters the quark mass,  $m_c$ ,  $a_c$ , and  $\mu_c$  related with the confinement strength and the strong coupling constant,  $\alpha_s$ . We define the

$$\chi^2(\vec{p}) = \sum_i \frac{(M_{\text{exp}}(i) - M_{\text{the}}(i, \vec{p}))^2}{\sigma_{\text{exp}}(i)^2}, \quad (D1)$$

where  $\vec{p}$  represents our model parameters and the experimental data are taken as  $M_{\psi(2S)} = 3686.093 \pm 0.143$  MeV,  $M_{\psi(3S)} = 4039.6 \pm 42.25$  MeV, and  $M_{\psi(4S)} = 4361 \pm 37$  MeV, where as explained previously the errors are taken as the half-width of the state. By minimizing the  $\chi^2$  function we obtain the theoretical uncertainties from the corresponding covariance matrix at the minimum. The outcoming values for the parameters are

$$\begin{aligned}
 m_c &= 1862 \pm 12.6 \text{ MeV} (0.68\%), \\
 a_c &= 524 \pm 43 \text{ MeV} (8.2\%), \\
 \mu_c &= 88 \pm 7.2 \text{ MeV} \quad (8.2\%), \\
 \alpha_s &= 0.41 \pm 0.14 (34\%),
 \end{aligned}
 \tag{D2}$$

where we put in parenthesis the relative uncertainties in percentage. Here we clearly see that the highest uncertainty corresponds to the value of the strong coupling constant. This rather large insensitivity to the otherwise too large  $\alpha_s$

is a rewarding feature of the renormalization approach. Actually, quite natural values of  $\alpha_s$  are obtained. The spectrum at the  $\chi^2$ -minimum is given by

$$\begin{aligned}
 \psi(2S) &= 3687 \pm 80 \text{ MeV}, \\
 \psi(3S) &= 4108 \pm 79 \text{ MeV}, \\
 \psi(4S) &= 4348 \pm 80 \text{ MeV}, \\
 \psi(5S) &= 4586 \pm 66 \text{ MeV}.
 \end{aligned}
 \tag{D3}$$

- 
- [1] E. Eichten, K. Gottfried, T. Kinoshita, K. D. Lane, and T.-M. Yan, *Phys. Rev. D* **21**, 203 (1980).
  - [2] D. B. Lichtenberg, *Int. J. Mod. Phys. A* **2**, 1669 (1987).
  - [3] M. B. Voloshin, *Prog. Part. Nucl. Phys.* **61**, 455 (2008).
  - [4] S. Godfrey and N. Isgur, *Phys. Rev. D* **32**, 189 (1985).
  - [5] S. Titard and F. J. Yndurain, *Phys. Rev. D* **49**, 6007 (1994).
  - [6] S. Titard and F. J. Yndurain, *Phys. Rev. D* **51**, 6348 (1995).
  - [7] G. S. Bali, *Phys. Rep.* **343**, 1 (2001).
  - [8] A. V. Smirnov, V. A. Smirnov, and M. Steinhauser, *Phys. Rev. Lett.* **104**, 112002 (2010).
  - [9] C. Anzai, Y. Kiyo, and Y. Sumino, *Phys. Rev. Lett.* **104**, 112003 (2010).
  - [10] M. Beneke, *Phys. Rep.* **317**, 1 (1999).
  - [11] N. Brambilla, A. Pineda, J. Soto, and A. Vairo, *Rev. Mod. Phys.* **77**, 1423 (2005).
  - [12] A. Pineda and J. Soto, *Nucl. Phys. B, Proc. Suppl.* **64**, 428 (1998).
  - [13] N. Brambilla, A. Pineda, J. Soto, and A. Vairo, *Nucl. Phys. B* **566**, 275 (2000).
  - [14] M. Beneke, *Phys. Lett. B* **434**, 115 (1998).
  - [15] A. Laschka, N. Kaiser, and W. Weise, *Phys. Rev. D* **83**, 094002 (2011).
  - [16] C. Bachas, *Phys. Rev. D* **33**, 2723 (1986).
  - [17] S. Nussinov, *Phys. Rev. Lett.* **86**, 4762 (2001).
  - [18] T. Burch *et al.*, *Phys. Rev. D* **81**, 034508 (2010).
  - [19] S. Bethke, *Eur. Phys. J. C* **64**, 689 (2009).
  - [20] Y. Koma, M. Koma, and H. Wittig, *Phys. Rev. Lett.* **97**, 122003 (2006).
  - [21] Y. Koma and M. Koma, *Nucl. Phys. B* **769**, 79 (2007).
  - [22] Y. Ikeda and H. Iida, [arXiv:1102.2097](https://arxiv.org/abs/1102.2097).
  - [23] T. Kawanai and S. Sasaki, *Phys. Rev. Lett.* **107**, 091601 (2011).
  - [24] Y. Koma and M. Koma, *Proc. Sci., LAT2009* (2009) 122 [[arXiv:0911.3204](https://arxiv.org/abs/0911.3204)].
  - [25] J. Vijande, F. Fernández, and A. Valcarce, *J. Phys. G* **31**, 481 (2005).
  - [26] E. Ruiz Arriola, A. Calle Cordon, and M. Pavon Valderrama, *econf C070910*: 161 (2007).
  - [27] M. Pavon Valderrama and E. R. Arriola, *Phys. Rev. C* **74**, 054001 (2006).
  - [28] E. R. Arriola and A. C. Cordon, *EPJ Web of Conferences* **3**, 02005 (2010).
  - [29] S. Necco and R. Sommer, *Nucl. Phys. B* **622**, 328 (2002).
  - [30] O. Alvarez, *Phys. Rev. D* **24**, 440 (1981).
  - [31] J. F. Arvis, *Phys. Lett. B* **127**, 106 (1983).
  - [32] A. Galindo and P. Pascual, *Quantum Mechanics* (Springer, New York, 1991).
  - [33] D. R. Entem, E. Ruiz Arriola, M. Pavon Valderrama, and R. Machleidt, *Phys. Rev. C* **77**, 044006 (2008).
  - [34] A. Calle Cordon and E. Ruiz Arriola, *Phys. Rev. C* **81**, 044002 (2010).
  - [35] M. Donnellan, F. Knechtli, B. Leder, and R. Sommer, *Nucl. Phys. B* **849**, 45 (2011) [arXiv:1012.3037](https://arxiv.org/abs/1012.3037).
  - [36] M. Pavon Valderrama and E. Ruiz Arriola, *Phys. Rev. C* **72**, 054002 (2005).
  - [37] C. Anzai, Y. Kiyo, and Y. Sumino, *Nucl. Phys. B* **838**, 28 (2010).
  - [38] J. Segovia, A. M. Yasser, D. R. Entem, and F. Fernandez, *Phys. Rev. D* **78**, 114033 (2008).
  - [39] K. Nakamura *et al.* (Particle Data Group), *J. Phys. G* **37**, 075021 (2010).
  - [40] X. L. Wang *et al.* (Belle Collaboration), *Phys. Rev. Lett.* **99**, 142002 (2007).
  - [41] G. Pakhlova *et al.* (The Belle Collaboration), *Phys. Rev. Lett.* **101**, 172001 (2008).
  - [42] R. Barbieri, R. Gatto, R. Kögerler, and Z. Kunszt, *Phys. Lett. B* **57**, 455 (1975).
  - [43] M. B. Voloshin, *Prog. Part. Nucl. Phys.* **61**, 455 (2008).
  - [44] W. Lucha, F. F. Schoberl, and D. Gromes, *Phys. Rep.* **200**, 127 (1991).
  - [45] M. Luscher and P. Weisz, *J. High Energy Phys.* **07** (2002) 049.
  - [46] G. Lambiase and V. V. Nesterenko, *Phys. Rev. D* **54**, 6387 (1996).
  - [47] V. V. Nesterenko and I. G. Pirozhenko, *Phys. Rev. D* **55**, 6603 (1997).
  - [48] G. Perez-Nadal and J. Soto, *Phys. Rev. D* **79**, 114002 (2009).
  - [49] D. B. Leinweber, *Nucl. Phys. A* **470**, 477 (1987).
  - [50] N. Brambilla, P. Consoli, and G. M. Prosperi, *Phys. Rev. D* **50**, 5878 (1994).
  - [51] N. Brambilla, A. Pineda, J. Soto, and A. Vairo, *Phys. Rev. D* **63**, 014023 (2000).
  - [52] N. Brambilla, D. Gromes, and A. Vairo, *Phys. Rev. D* **64**, 076010 (2001).
  - [53] W. Frank, D. J. Land, and R. M. Spector, *Rev. Mod. Phys.* **43**, 36 (1971).